The future of PSMA-PET and WB-MRI as next generation imaging tools in prostate cancer

Yishen Wang[1,2], Joao R Galante[3], Athar Haroon[4], Simon Wan[5], Asim Afaq[5,6], Heather Payne[7], Jamshed Bomanji[5], Sola Adeleke[7,8]* & Veeru Kasivisvanathan[9,10]*

1. School of Clinical Medicine, University of Cambridge, Cambridge United Kingdom
2. Barking, Havering and Redbridge University Hospitals NHS Trust, Romford United Kingdom
3. Dept of Oncology, Guy's & St Thomas' NHS Foundation Trust, London United Kingdom
4. Department of Nuclear Medicine, Barts Health NHS Trust, London United Kingdom
5. Institute of Nuclear Medicine, University College London, London United Kingdom
6. Department of Radiology, University of Iowa Carver College of Medicine, Iowa City, Iowa United States of America.
7. Department of Oncology, University College London Hospitals, London United Kingdom
8. School of Cancer & Pharmaceutical Sciences, King's College London, Strand, London United Kingdom,
9. Division of Surgery & Interventional Science, University College London, London United Kingdom.
10. Department of Urology, University College London Hospitals NHS Foundation Trust, London United Kingdom

**These authors share joint senior authorship.*

Abstract

Radiolabelled prostate-specific membrane antigen (PSMA)-based Positron emission tomography-computed tomography (PET-CT) has been shown in numerous studies to be superior to conventional imaging in the detection of nodal or distant metastatic lesions. ^{68}Ga-PSMA PET-CT is now recommended by many guidelines for the detection of biochemically relapsed disease after radical local therapy. PSMA radioligands can also function as radiotheranostics, namely Lu-PSMA has been shown to be a potential new line of treatment for metastatic castrate resistant prostate cancer. W hole-body MRI (WB-MRI) has been shown to have a high diagnostic performance in the detection and monitoring of metastatic bone disease. Prospective, randomized, multi-centre studies comparing ^{68}Ga-PSMA PET-CT and WB-MRI for pelvic nodal and metastatic disease detection are yet to be performed. Challenges for interpretation of PSMA include tracer trapping in non-target tissues and urinary excretion of tracers confounding image interpretation at the vesicoureteral junction. Additionally , studies have described how long-term androgen deprivation therapy (ADT) affects PSMA expression and could, therefore, reduce tracer uptake and visibility of PSMA-positive lesions . Furthermore, ADT of short duration might increase PSMA expression, leading to the PSMA flare phenomenon, which makes it challenging to accurately monitor treatment response to ADT with PSMA-PET. Scan duration, detection of incidentalomas and presence of metallic implants are some of the major challenges with WB-MRI. Emerging data supports the wider adoption of PSMA-PET and WB-MRI for diagnosis, staging, disease burden evaluation and response monitoring, though their relative roles in the standard of care management of patents is yet to be fully defined. .

Key points

- Next-generation imaging techniques have been found to affect prostate cancer disease state classifications as their increased sensitivity can result in stage migration.

- PSMA-PET has been shown to have higher sensitivity and specificity in detecting nodal and metastatic lesions than conventional imaging. PSMA-derived tumour volume (PSMA-TV) and total lesion PSMA (TL-PSMA) are experimental quantitative volumetric measures for whole-body tumour burden with good prognostic value for progression-free survival and can be used in treatment response assessment.
- ^{177}Lu-labelled PSMA is a potential new line of therapy in patients with metastatic castration-resistant prostate cancer (mCRPC) who have progressed on at least one line of chemotherapy.
- WB-MRI is showing increasing promise as an 'all-in-one' modality for cancer diagnosis and staging without the need for radiation exposure. WB-MRI-derived markers include apparent diffusion coefficient (ADC), Signal fat fraction (sFF) and proton density fat fraction (PDFF). ADC values are especially useful for assessing bone metastases; PDFF and sFF are emerging quantitative imaging biomarkers that might be useful in assessing nodal and bone marrow metastases.
- Limitations of PSMA-PET include tracer trapping in non-target tissue, PSMA flare phenomenon, limited availability and radiation exposure related to radiotracers. Limitations of WB-MRI include long acquisition time, metal-related and motion-related artefacts, fat–water swapping, incidentalomas, differential diagnoses of findings and limited availability.
- Well-designed, powered, randomized multi-centre studies are needed to assess the value of PSMA-PET, WB-MRI and standard imaging for disease detection, disease burden evaluation and survival across different prostate cancer disease states.

[H1]Introduction

Prostate cancer is the second most common cancer in men globally, with more than 1.4 million men (14.1% of new cancer cases) diagnosed in 2020 and is one of the major causes of cancer-related mortality worldwide[1]. The initial presentation of prostate cancer is categorized into a number of disease states based on tumour characteristics as evidenced on digital rectal examination, Gleason score and serum PSA measurement[2]. These parameters enable categorization of prostate cancer into localised, locally advanced and metastatic disease. The metastatic disease state can be subdivided into oligometastatic and poly-metastatic groups[3] Biochemical classification based on testosterone levels being in the normal range (hormone-sensitive disease) or low (castration-resistant disease) levels is also an important stratifier[4] Hormone-sensitive disease that is initially responsive to ADT can progress to a refractory state: castration-resistant prostate cancer (CRPC)[5] 27-53% of those patients who initially present with localised prostate cancer will go on to develop biochemical recurrence (BCR) following local therapy, a disease state which predicts the development of subsequent overt metastatic disease and adverse survival outcome[6]

Accurate diagnosis and evaluation of disease burden are essential for early planning of treatment strategies to ensure the best possible outcomes. Unfortunately, conventional imaging tools such as CT and bone scan which are used for primary staging, detection of recurrent and metastatic disease and response assessment, have several limitations, including low sensitivity to detect small-volume disease and the inability to differentiate between osteoblastic healing and early disease progression in bone lesions (also known as flare phenomenon)[7] . Several advanced imaging techniques have now emerged and evidence for their use is maturing. Collectively termed 'next generation imaging (NGI)' in the uro-oncology community, these techniques are now being translated into clinical routine to fulfil the unmet need for better accuracy for disease detection and response evaluation.

WB-MRI and PSMA-PET are two potential forerunners in NGI for prostate cancer, both of which are increasingly available in clinical practice. WB-MRI and PSMA-PET have overlapping (generally whole-body) coverage and the potential to provide comprehensive disease assessment of the prostate, pelvis, nodal and other distant sites, with incremental value beyond conventional imaging. Indeed, in other tumour contexts such as non-small cell lung cancer, colorectal cancer and multiple myeloma, WB-MRI and PET (using an FDG tracer) have been compared against each other with respective accuracy scrutinised [8,9,10]. The Streamline L and Streamline C trials are two multicentre trials comparing the diagnostic accuracy of WB-MRI as a one-step staging modality versus the standard staging pathway (which includes a combination of CT, MRI PET CT and biopsy) in newly diagnosed non-small cell lung cancer(NSCLC) and colorectal cancer respectively. Data from Streamline L for newly diagnosed NSCLC showed that WB-MRI has higher sensitivity compared to standard staging pathway (54% vs 50%), has a similar agreement rate with the MDT team's final decisions (99% vs 98%), requires less time to complete staging compared to standard pathway(13 days vs 19 days) and is more cost-effective (mean cost per patient was £317 vs £620)[8]. Similarly, the Streamline C trial[9] showed that WB-MRI is more sensitive compared to standard messpathways (67% vs 63%) in newly diagnosed colorectal cancer and requires a shorter staging time (8 days vs 13 days) and costs(£216 vs £285). The data regarding imaging of prostate cancer is evolving, and experience and evidence with both WB-MRI and PSMA PET are accumulating. An in-depth understanding of both techniques might help individual clinicians and centres to navigate the choice of imaging techniques until a definitive and clear consensus can be achieved.

In this article, we review the current evidence for the use of PSMA-PET and WB-MRI, describing their current uses across various disease states in prostate cancer and how the limitations of each modality could affect clinical decision-making. Furthermore, we consider the evolving use of PSMA-PET-derived and WB-MRI-derived quantitative biomarkers and attempts made at their standardisation. In addition to the diagnostic aspects of NGI, PSMA-PET has additional benefits as a potential predictive marker for efficacy and response evaluation using Lu-177 PSMA radionuclide therapy, which has shown early promise. Finally, we make recommendations for future clinical trials that could generate high-level evidence for adoption of these imaging modalities into routine clinical practice.

[H1]Roles of NGI in various settings

The following section provides an overview on the roles of PSMA PET and WB-MRI in various disease states of prostate cancer.

[H2]Newly diagnosed high-risk disease

Diagnosis of localized or locally advanced disease is typically made based on PSA test, age-based screening or by patient request in men with a strong family history [11,12]. Before a decision is made regarding radical treatment particularly in high-intermediate risk patients, whole-body imaging is required to determine whether any nodal or distant metastases are present. Conventional imaging with CT and bone scan are known to be insufficient in assessing nodal or distant disease especially in patients with low serum PSA levels [13]. This means NGIs are now regarded as important imaging tools in guiding treatment options in this setting. . American Society of Clinical Oncology (ASCO) guidelines recommend the use of NGIs in the evaluation of high-risk locally advanced prostate cancer, in which conventional imaging is

negative, indeterminate or suspicious[14]. A number of studies[15-19] have shown that PSMA-PET outperforms conventional imaging in identifying nodal and metastatic bone disease, with up to 27% greater diagnostic accuracy (92% [88–95] versus 65% [60–69]; p<0·0001) compared with conventional CT and bone scan. In a 2020 systematic review including 18 trials and 969 patients assessing PSMA PET for primary lymph node staging[18], the weighted sensitivity, weighted specificity and positive predictive values were 59%, 93% and 20-100% (greater than 80% in the majority of trials), respectively (compared with 42%, 82% and 32% for CT). Studies have shown that WB-MRI provides a high level of diagnostic accuracy for both nodal and metastatic bone disease, with a higher sensitivity to detect bone metastases than bone scan and performs as well as ^{18}F-choline PET/CT[20,21]. The reported mean sensitivity and specificity of WB-MRI for N1 disease were 100% and 96%, respectively, compared with 100% and 82% for ^{18}F-choline PET/CT, whereas for M1b disease the mean sensitivity and specificity of WB-MRI, ^{18}F-choline PET/CT, and bone scan were 90% and 88%, 80% and 92%, and 60% and 100%, respectively[20].

[H2]Biochemical recurrence

^{68}Ga-PSMA has established itself as the optimal imaging tool for diagnosis in the biochemical relapse (BCR) and biochemical persistence settings after radical local treatment. The modality has gained USA FDA approval for its use in the investigation of BCR after radical prostatectomy or radiotherapy, and many national and international guidelines typically recommend it in this setting. Despite these developments, ^{68}Ga-PSMA might not be readily accessible in many hospital practices , as regulatory requirements in different geographical regions affect the availability of tracers. Although ^{68}Ga is used for other clinical indications, such as detection of neuroendocrine tumours, availability of the ^{68}Ga PSMA tracer is not ubiquitous. Instead, validation of ^{18}F-PSMA which is more available might help alleviate the accessibility concerns with ^{68}Ga-PSMA. One major requirement for ^{68}Ga is the need for an onsite generator for its production. The longer half-life of ^{18}F (approximately 110 minutes) compared with ^{68}G (approximately 68 minutes) makes central production and then distribution of ^{18}F PSMA tracers to sites without a cyclotron much easier[22].

The detection rate of biochemically recurrent prostate cancer using PSMA-PET following primary radiotherapy varies with serum PSA levels: detection rate is 77.8% for PSA 0.5–<1.0 ng/ml, 76.7% for PSA 1–<2.0 ng/ml, and 90.6% for PSA >2.0 ng/ml[23]. The use of ^{68}Ga-PSMA-PET for detection of biochemical recurrence in patients whom ^{18}F-choline-PET did not demonstrate recurrent disease revealed detection rates of 28.6%, 45.5%, and 71.4% for serum PSA levels of ≥0.2–1 ng/mL, 1–2ng/mL and >2 ng/ml, respectively[24]. In a study comparing WB-MRI and ^{68}Ga-PSMA PET-CT following radical prostatectomy, ^{68}Ga-PSMA PET-CT detected 56 of 56 lesions (100%) in 20 of 28 patients with biochemical recurrence (71.4%), whereas WB-MRI detected 13 lesions (23.2%) in 11 of 28 patients (39.3%)[25]. Results of the LOCATE[26] trial evaluating the diagnostic accuracy of WB-MRI in BCR following radiotherapy are imminent

[H2]Oligometastatic disease

The oligometastatic disease state has been shown to have a more favourable outcome following metastasis-directed therapy (MDT) than poly-metastatic disease [27,28,29,30]. No consensus definition of oligometastatic prostate cancer is available; however, the most commonly accepted definitions of oligometastatic disease include the presence of three or fewer, four or fewer, or five or fewer metastatic or recurrent lesion,[31,32,33] that could be treated by local therapy to improve prognosis. The various definitions also disagree on the types and/or numbers of involved organ sites. Commonly used criteria are based on large clinical trials such as the CHAARTED trial[34], which classifies individuals with ≥4 bone metastases (at least 1 in the non-axial skeleton) or visceral metastases as having a high metastatic burden,

whereas all others are classified as having a low metastatic burden. CHAARTED definition is commonly used due to the need for less clinical information to arrive at a determination of disease volume.

Results from many studies have shown the efficacy of metastasis-directed therapy (MDT) in patients with oligometastases. For example, the SABR-COMET trial[27] is a multicentre, randomised trial involving 99 patients with a controlled primary malignancy (breast, lung, colorectal, prostate or other types) and 1–5 oligometastases randomised to receive MDT with stereotactic ablative body radiotherapy (SABR) to all metastatic sites or palliative radiotherapy. The results from SABR-COMET demonstrated that patients who received SABR had longer median survival (41 months versus 29 months) compared to patients who received palliative radiotherapy. However, only a subset (16 out of 99) of patients in the SABR-COMET trial[27] had prostate cancer. Outcomes from the STOMP trial[28], which compared MDT versus surveillance in 62 patients with biochemical recurrence following primary prostate cancer with curative intent and three or fewer asymptomatic, extracranial metastases also demonstrated that MDT using either surgery or SABR significantly improved 5-year ADT-free and CRPC-free survival compared with surveillance alone. An evaluation of the national SABR service in the UK, in which 28.6% of patients had prostate cancer, showed that patients with various primary solid organ cancers and ≤3 extracranial metastatic lesions who had MDT had a high overall survival (OS 92.3% at 1 year)[29]. Furthermore, data from the ORIOLE study[30], which involved 52 men with recurrent hormone sensitive prostate cancer with oligometastases (1 to 3 metastases) who had not received ADT within 6 months randomised to receive SABR or observation only, showed that 19% of patients who had MDT with SABR had progression at 6 months compared with 61% in the observation group *(p*=0.005). To date, no prospective study of WB-MRI-guided MDT for oligometastatic prostate cancer has been reported in the literature.

Studies of the use of SABR for the treatment of oligometastatic disease with higher disease burden(4-10 lesions) that use NGI for patient selection are ongoing[27]. Future randomized trial designs have been proposed whereby patients identified as having M0 disease on conventional imaging are scanned with NGIs and, based on NGI reports, are classified into non-metastatic, oligometastatic and poly-metastatic disease states. Outcome measures of such studies could be metastasis-free survival (MFS) and overall survival.[35]

[H2]Management of metastatic disease

NGI seems to be increasingly used for monitoring in metastatic disease, despite a lack of prospective randomised clinical trials showing outcome benefits over conventional imaging[36]. Even so, they could have an important role in this scenario, especially when they are performed at baseline. NGIs could facilitate future comparison and disease assessment or be valuable when a change in treatment might be imminent owing to clinical suspicion but when conventional imaging is equivocal. Although clinical parameters such as PSA or established criteria such as RECIST are still standard tools used in the clinic, PSA might not accurately predict response in some patients, especially in PSA-non-secreting disease[37]. Application of RECIST criteria is often hampered by the requirement for presence of bone metastases with soft tissue components measuring ≥ 10 mm on conventional imaging[38,39].

The few studies that have reported using NGI for response assessment are either retrospective or are very small, unpowered feasibility studies. For example, a retrospective study that assessed concordance in treatment response between PSA and ^{68}Ga-PSMA, between PSA and CT, and between ^{68}Ga-PSMA and CT in 23 patients showed that concordance was 56%, 33% & 58%, respectively, in predicting treatment outcome[40]. A 2014 study of patients with bone metastases from primary breast or prostate tumours (n=7) assessed treatment response to various anti-cancer therapies with semi-automatic segmentation of

whole-body diffusion-weighted imaging using a Markov random field model. Responding patients demonstrated a larger increase in global ADC (median +0.18, range -0.07 to +0.78×10−3 mm2/s) after treatment than non-responding patients (median change -0.02, range -0.10 to +0.05×10−3 mm2/s, $p = 0.05$[41]. Further prospective data regarding the role of NGIs in the management of metastatic disease are required. PET and MRI might enable disease quantification and categorisation[42], for instance into 'complete responders', 'partial responders' or 'stable disease' based on age-standardised imaging interpretation tools. This approach might provide more objective disease assessment or quantifiable assessment of therapeutic benefit than interpreting images without standardised protocols which are subject to interobserver variability. Such disease or response quantification steps are already being taken in diseases such as multiple myeloma[43], in which WB-MRI or PET imaging have important roles.

[H1]PSMA tracers used in prostate cancer

PSMA is a type II membrane glycoprotein (100-120kDa) that is expressed 100–1,000-fold higher in prostatic adenocarcinoma than other PSMA-expressing tissues, such as the benign prostate, kidney, proximal small intestine or salivary glands, making it a valuable clinical biomarker of prostate cancer[44]. As described in table 1, small molecules, antibodies and antibody fragments that target PSMA have been generated and radiolabelled for molecular imaging. This includes ^{68}Ga-labelled PSMA tracers, such as ^{68}Ga-PSMA-HBED-CC (also known as ^{68}Ga-PSMA-11), ^{68}Ga-PSMA-617 and ^{68}Ga-PSMA I&T. Others include ^{18}F-labelled PSMA tracers, such as ^{18}F-DCFPyL, ^{18}F-DCFBC and ^{18}F-PSMA-1007, and ^{64}Cu-PSMA-617[45]. Among these, the ^{68}Ga-HBED-CC ligand is one of the most widely used PSMA PET tracers. Its structure is based on a urea backbone, and it binds to the extracellular domain of PSMA with high affinity, after which it is efficiently internalized[46]. ^{68}Ga-PSMA-11 radiotracer uptake within normal organs is highest in kidney and salivary glands, whereas the spleen, liver, lacrimal gland and bowel show moderate uptake[47]. A growing body of evidence supports the use of ^{68}Ga-PSMA-11 both in preoperative staging and evaluation of biochemical recurrence following primary therapy.

In primary staging, identification of metastatic disease is crucial for treatment decision planning and prognosis. The commonest sites for extraprostatic spread are lymph nodes and bone[48]**.**Traditionally, imaging tools such as CT and Tc-99m bone scintigraphy have an important role in the initial staging of prostate cancer, although they are unlikely to yield any diagnostic information in patients with prostate cancer who are clinically asymptomatic for bone metastasis and have serum PSA ≤20.0ng/ml[49]. Introduction of PET/CT using tracers such as ^{18}F-choline or ^{11}C-choline offer increased imaging resolution and diagnostic confidence to rule out metastatic disease; however, their sensitivity and specificity profile remain suboptimal at low PSA levels both for diagnosis and response monitoring, with a reported detection rate of 36% in patients with PSA < 1 ng/ml[50].

PSMA-PET is superior to conventional imaging at identifying both nodal disease[16,17,18,19] and bone metastases[51]. Its promising clinical utility is further supported by results from the proPSMA trial, which involved 302 men with high-risk localised prostate cancer who were randomly assigned to imaging using ^{68}Ga-PSMA-PET or conventional imaging techniques (CT plus bone scan). PSMA-PET had higher sensitivity (85% versus 38%) and specificity (98% versus 91%) than conventional imaging at detecting pelvic nodal and distant metastatic disease, and consequently more often prompted a change in treatment intent[15].

Unlike conventional imaging tools, PSMA PET has been demonstrated to be particularly suitable to detect recurrences owing to its ability to detect lesions that might be amenable to therapy, even when serum PSA is very low. In a 2018 meta-analysis[52], the pooled detection rate of PSMA-PET was 50% with a restaging PSA as low as 0.2-0.49 ng/ml; however, the detection rate increased with increased PSA levels[53]. ^{68}Ga-PSMA has higher sensitivity and specificity profiles than choline-based tracers at all PSA levels in the biochemical recurrence setting [54,55.] Thus, the EAU guidelines recommend using ^{68}Ga-PSMA PET (if available) or fluciclovine or choline PET in patients with biochemical recurrence at low serum PSA levels (PSA<1ng/L).

Subsequently, novel second-generation PSMA probes including ^{18}F-DCFPyL, ^{18}F-PSMA-1007 and [^{68}Ga] THP-PSMA have demonstrated superiority to conventional imaging at detecting metastases (Table 1). Ongoing trials[56,57] are assessing the performance of these novel PSMA tracers at diagnosis, staging and detecting metastatic disease.

[H1]PSMA-derived biomarkers

Quantitative image biomarkers derived from PSMA PET include molecular tumour volume (PSMA-TV) and total lesional PSMA expression (TL-PSMA), which provide a useful measurement of the total tumour burden with prognostic value and can assist clinical decision making across all prostate cancer stages.

[H2]PSMA-derived tumour volume and total lesion PSMA.

Molecular tumour volume (PSMA-TV) is a biomarker derived from PSMA PET imaging and is defined as the sum of all PSMA-avid lesions with standard uptake value (SUV) ≥ 3, in which SUV is a quantitative measurement of PSMA tracer uptake. Total lesional PSMA expression (TL-PSMA) is calculated as the product of PSMA-TV and SUV_{mean} (PSMA-TV×SUV_{mean}). These values are quantitative volumetric measurements of whole-body tumour burden and are useful parameters to assist clinical decision-making across all prostate cancer stages. A study of 88 patients undergoing initial staging for prostate cancer reported a moderate correlation between serum PSA and PSMA-TV and a high correlation between TL-PSMA and serum PSA[58]. Other studies have shown that both PSMA-TV and TL-PSMA correlate well with Gleason score and are good predictors of progression-free survival [59,60,61]. PSMA-TV and TL-PSMA have also been shown to be beneficial in the context of treatment response assessment, in which changes in both parameters are concordant with PSA changes (biochemical response) following treatment[62,63,64,65] In a study of 19 prostate cancer patients treated with Lu-177 PSMA I&T, PSMA-TV values were decreased in 12 patients (63%), and TL-PSMA values were decreased in 15 patients (79%) following treatment. Accordingly, the SUVmax and the PSA values also decreased in 14 (74%) and 10 (53%) patients, respectively[62]. However, follow-up data in patients with PSMA-TV are lacking. Moreover, histological assessment of PSMA-avid lesions that enables correlation with PSMA-derived volume measurement is not feasible in all cases due to ethical issues and patient distress related to invasive biopsy procedure particularly in relapse settings where repeat biopsies are not often clinically indicated as their results would not affect clinical management. Thus, these approaches remain in their infancy and further prospective trials are needed to reveal the full potential of these PSMA-PET-derived parameters.

[H1]Standardized imaging interpretation tools

Agreement on standards of interpretation and processing of PSMA PET images is required to ensure consistent quality and reproducibility of reporting to support clinical decision making or for the radiological findings to be used in research and clinical trials. Standardized imaging interpretation tools such as PERCIST, PROMISE, PSMA-RADS and E-PSMA have been proposed for this purpose.

[H2]PERCIST, PROMISE and PSMA-RADS

PET response criteria in solid tumours (PERCIST) is a group of molecular criteria that were initially formulated for response evaluation of fluorodeoxyglucose PET-CT (FDG PET-CT)[66] (Box 1). The creation of these criteria aimed to address the limitations of anatomical tumour response metrics such as RECIST — for instance, potential loss of valuable information by reducing continuous tumour information into four categories (complete response, partial response, stable or progressive disease) – and enabling quantitative assessment of PET response.

The PERCIST criteria have been specifically adapted for PSMA PET response evaluation[67], showing that for ^{68}Ga-PSMA PET-CT response evaluation, molecular criteria outperformed morphological criteria in patients with metastatic prostate cancer with PSA progression. In particular, a drop of ≥30% in the highest SUV_{max} was considered a partial response; a ≥30% increase was considered progressive disease and the detection of a new PSMA-avid lesion was also considered as progressive disease. Similar to the original PERCIST 1.0, detected changes between partial response and progressive disease were considered as stable disease (or stable metabolic disease)

PERCIST has been evaluated in a number of FDG-PET trials but is yet to be validated in prostate PSMA studies. A reason for this omission might be because the patterns of tracer uptake on PSMA scans are different from the FDG-PET scans as PSMA is a receptor-based tracer, unlike FDG-PET, which shows metabolic changes. Concerns around incidental physiological uptake that could sometimes be mistaken for disease have led experts in the field to consider the design of standardized reporting and interpretation systems for PSMA. One of these systems — Prostate Cancer Molecular Imaging Standardized Evaluation (PROMISE) — is proposed for use in staging and the other system — PSMA reporting and Data system (PSMA-RADS) — is proposed for use in lesion characterisation. PROMISE assigns a visual scoring system (0-3) relative to SUV in liver and blood pool, whereas PSMA-RADS applies scores 1-5 where 1 signifies normal tissue or a benign lesion and 5 indicates a malignant lesion with a high certainty[68]. Neither of these tools has yet been tested in multicentre randomised studies.

[H2]E-PSMA

E-PSMA is a standardised PSMA reporting guideline supported by the European Association of Nuclear Medicine, which contains consensus statements proposed by selected panellists consisting of PSMA-PET experts worldwide[69]. E-PSMA provides guidance on the standard reporting of suspected prostate cancer sites by region including prostate, prostatic bed, and metastasis (lymph nodes, bone, or visceral soft tissue), as well as the reporting of PSMA-PET imaging in various prostate cancer settings: primary staging, recurrent setting, advanced setting, and assessment of treatment response to systemic therapy. Implementation of E-PSMA could contribute to uniform and reproducible image interpretation, which should lead to more consistent reporting in clinical practice and increased data reproducibility in clinical trials. The E-PSMA criteria has been applied as the reporting criteria in some clinical studies[70,71], however more robust validation of the criteria is awaited.

[H1]Limitations of PSMA PET

Although PSMA-PET performs well for detecting metastases in prostate cancer, it does have some pitfalls and limitations that complicate its implementation in evaluation of disease burden and assessment of treatment response The effects of these limitations mentioned could complicate interpretation of PSMA-PET imaging in general, however especially for the scenario of treatment response assessment to ADT – explained below.] . These include tracer trapping, PSMA flare, radiation exposure and limited availability.

[H2]Tracer trapping.

Tracer trapping refers to the accumulation of tracer activity in non-target tissue — in the case of PSMA PET, some normal tissue also expresses PSMA receptors, which could, therefore, show tracer activity during imaging, resulting in false positive findings. For example, the coeliac and stellate sympathetic ganglia can exhibit sufficient PSMA tracer uptake such that they can mimic lymph node metastases[72,73]. Various benign lesions can also display vivid tracer uptake, including bone-related conditions such as fibrous dysplasia[74] and healing fractures[75]; benign tumours such as thyroid adenomas[76] and desmoid tumours; and pulmonary inflammation and infections[74]. A variety of malignant neoplasms also express PSMA, such as renal cell carcinoma, lung cancer, CNS glioma, gastric and pancreatic adenocarcinomas[74]. Such lesions are rarely misinterpreted as metastases as these are very atypical sites, but they can occasionally be challenging for physicians to ascertain whether they represent a synchronous pathology. Detection of cancer recurrence at the prostate bed, which is fundamentally important for treatment response monitoring, is also complicated by the accumulation of tracer in the bladder and urethra, and, in patients who have received high-intensity focused ultrasound (HIFU), in the cavities formed from the therapy. MRI has been found to provide better structural information on the prostate bed than PSMA-PET.[77]

[H3]Tracer excretion in the urine.

Urinary excretion is the major elimination pathway for most PSMA PET tracers. Thus, excreted radiotracer activity in the ureters can confound interpretation of small retroperitoneal and pelvic lymph nodes close to the ureters. In BCR settings, intense radiotracer activity in the urinary bladder can obscure the evaluation at the vesicourethral junction[78], which is particularly problematic given that this is the most frequent site for local recurrence. The use of tracers with lower urinary excretion could be used to counter this. For instance, 18F-rhPSMA-7 has been shown to have a higher tumour-to-bladder ratio than 68Ga-PSMA-11, including in cases with local recurrence[79]. F-PSMA-1007 with liver-dominant excretion has been shown to increase confidence of diagnosing small locoregional lesions adjacent to the urinary tract compared with other PSMA tracers[80]. However, in both studies, the test agents were associated with increased detection of falsely PSMA-positive lesions elsewhere, which were deemed to be benign or non-specific by experts, particularly in the skeleton. Switching of the tracer type might, therefore, introduce other errors and difficulties with longitudinal comparison. Moreover, availability of these specific tracers is limited for some centres due to variations in licensing, commissioning and supply chain constraints.

Other strategies have also been attempted to overcome the challenge of urinary excretion, including the use of diuretics such as furosemide[81], the urographic (delayed)[82,83] phase of iodinated contrast CT, dual point PET imaging (to look for persistent PET-avid lesions at the bladder neck)[84] or early dynamic PET imaging (to capture early tracer perfusion and avidity in local recurrent disease prior to arrival of excreted urinary tracer activity) in some centres [85,86]. Correlation of PSMA PET findings with mpMRI, including the use of integrated PET-MRI

platforms might also be useful[87,88]. These approaches have been met with variable success, but confident diagnosis of vesicourethral junction recurrence remains a challenge (Fig. 1; Fig. 2)

[H2]PSMA flare and false positive uptake.

I*n vitro* studies[89] and data from mouse xenograft models[90] have shown that cellular PSMA expression is quantitatively increased by short-term androgen depletion. This phenomenon has been confirmed in human patients by the work of Hope et al. In one patient with castration sensitive metastatic prostate cancer, PSMA PET Imaging demonstrated an increase in ^{68}Ga-PSMA-11 SUV_{max} from 2.9 ± 3.0 to 11.8 ± 6.9 (707% ± 689%) across 22 measurable lesions ($P < 0.001$) 4 weeks after initiation of ADT. [91]. The upregulation of PSMA expression is evident even in androgen-independent prostate cancer cell lines that are refractory to treatment with antiandrogens[92]. However, *in vivo* animal studies show that while the amount of PSMA per cell increased, the overall size of the tumour decreased in response to castration and enzalutamide[90]. Thus, PSMA uptake on imaging does not necessarily correspond with tumour size measurements, which can render treatment response monitoring challenging and less accurate in this setting.

Conversely, a study in humans of 31 metastatic prostate cancer lesions in 10 patients who were imaged with PSMA-PET before and after continuous long-term ADT treatment (mean 7 months, range 5 to 11 months) showed that PSMA uptake was significantly reduced in 71% and increased in 12.9% of the metastatic prostate cancer lesions after continuous ADT treatment[93]. Some studies have shown a significant association between a positive PSMA PET result (that is, detection of at least one lesion indicative of prostate cancer) and ADT[94,95], whereas others reported no significant change in detection efficacy[96]This difference could be due to the heterogeneity in study setup: some studies involved only hormone-sensitive[93] or castrate resistant prostate cancer patients[96] in analysis, while others included both groups[94,95]; the timing of PSMA PET imaging following initiation of ADT could also play a role - for instance, Emmett et al. detected a significant increase in SUV_{max} in castrate resistant prostate cancer patients after 9 days of initiating ADT which plateaued after day 28, whereas no PSMA flare phenomenon was reported on imaging by Plouznikoff et al. at a median follow up of 3 months, however an early and short lived flare cannot be excluded. Finally, the numbers of patients included in these studies were small .

Clearly, these findings have implications for the application of PSMA-PET in treatment-response monitoring for ADT. The exact effect of ADT on PSMA PET results is being elucidated by ongoing trials such as the ADTPSMA2 study[97], which compares the mean increase of SUVmax of prostate cancer lesions in 18F-PSMA 1007 PET before and 3 weeks after the initiation of GnRH antagonist in 35 men with newly diagnosed metastatic prostate cancer. The same cohort would undergo yearly follow-up PSMA PET scans until the time of progression to castrate-resistant prostate cancer. The study is estimated to be completed by March 2023.

PSMA expression in non-prostatic tissue could have a substantial effect on clinical decision making[74,98]. For example, a patient with known prostate cancer with PSMA scan that shows avidity in a lung nodule might be wrongly diagnosed as having pulmonary metastases (Fig. 3A-D), unless biopsy sampling is available to confirm whether the lung lesion is a squamous cell lung carcinoma. This result on PSMA PET could, therefore, affect patients without an opportunity for a histological confirmation. PSMA uptake in the stellate, coeliac and sacral ganglia can sometimes be difficult to differentiate from suspicious or avid cervical,

retroperitoneal or pelvic lymph nodes (Fig. 3e-k) [72,99]. These pitfalls should be recognised and mitigated as much as possible by corroborative data from other investigations where available.

[H2]Radiation exposure.

Inevitably, PSMA PET scans are associated with ionising radiation; the estimated dose of radiation for receiving one scan is 8·4 mSv, with the highest radiation received by the kidney[15]. As a comparison, the UK average background radiation dose experienced by an average person over a year is 2.7 mSv, with the majority (48%) originating from radioactive radon gas from the ground[100]. Although the dose associated with PSMA PET is much lower than what patients might have received from radiotherapy, the serial and longitudinal nature of follow-up imaging studies to assess treatment response mean the overall radiation dose received by patients from having the scans is not insignificant compared with modalities such as WB-MRI, which does not involve the use of ionising radiation..

[H1]PSMA theranostics in prostate cancer

In addition to providing high-quality, highly specific prostate cancer PET imaging, PSMA radioligands have also been used in targeted radionuclide therapy with encouraging results, which gives PSMA radioligands a unique added benefit compared with other non-PSMA based tracers such as ^{18}F FDG or ^{18}F Choline[101] .

In two large multicentre studies, [^{177}Lu]Lu-PSMA-617 (Lu-PSMA) has been shown to be a potential new line of therapy in patients with mCRPC who have progressed on at least one line of chemotherapy. The TheraP trial was a randomised phase 2 trial that compared Lu-PSMA with Cabazitaxel in 200 men with mCRPC[102] and recruited and triaged men based on their ^{68}Ga-PSMA PET status. Patients were admitted into the study if they had a SUV_{max} of >20 at a single site or SUVmax>10 other sites of measurable disease (size≥10mm. Patients with disease sites that have discordant FDG-positive and PSMA-negative findings were also excluded. The primary end point for the study was ≥50% reduction in PSA from baseline levels; PSA response was shown to be 66% in the Lu-PSMA arm versus 37% in the cabazitaxel arm (*p*= 0.0001).

A second study, VISION, was a phase 3 trial in 831 men that compared [^{177}Lu]Lu-PSMA-617 in men with mCRPC who have progressed on at least one line of androgen receptor pathway inhibitor agent and one or two taxane chemotherapy regimens[103]. Lu-PSMA was given with protocol-permitted standard of care (permitted treatments included but were not restricted to the approved hormonal treatments, bisphosphonates, radiation therapy, denosumab, or glucocorticoid at any dose but not chemotherapy, immunotherapy, radium-223 (223Ra), and investigational drugs due to the lack of safety data combining Lu-PSMA with these agents) and compared against patients who received standard of care alone. Alternate primary endpoints were imaging-based progression-free survival (PFS) and overall survival. Median PFS was 8.7 months in the Lu-PSMA arm versus 3.4 months for standard of care (HR 0.4, 99.2% CI 0.29 to 0.57, p<0.001). Median overall survival was 15.3 months in the Lu-PSMA arm versus 11.3 months for standard of care (95% CI 0.52 to 0.74, p<0.001).

With the high mortality rate of mCRPC patients being driven by resistance to hormonal therapy[103], a new line of therapy for this particular patient subset is needed. The results from

the TheraP and VISION trials demonstrated that Lu-PSMA is an effective new line of therapy for patients with mCRPC with a higher PSA response and longer overall survival compared to current standard of care.

The possibility of carrying out Lu-PSMA therapy without having a prior PSMA PET scan has also been considered as a possible management strategy. . In the VISION study, patients were eligible if they had at least one PSMA-positive metastatic lesion and no PSMA-negative lesions according to the protocol criteria [103]. A PSMA-positive lesion was defined as ^{68}Ga-PSMA-11 uptake greater than that of liver parenchyma in one or more metastatic lesions of any size, in any organ system; a PSMA-negative lesion was defined as uptake equal to or lower than that of liver parenchyma in any lymph node with a short axis of at least 2.5 cm; in any metastatic solid-organ lesions with a short axis of at least 1.0cm; or in any metastatic bone lesion with a soft-tissue component of at least 1.0 cm in the short axis[103]. Approximately 87% of patients met these criteria in VISION, meaning that the majority of the real-world mCRPC patient population would have met the criteria and benefited from treatment with Lu-PSMA even if pre-treatment PSMA scans were not performed to identify them. . Due to challenges with costs and availability of either tracer, some argue that PSMA scans might not be needed before Lu-PSMA therapy[104]. However, bypassing the pre-treatment PSMA PET scan would mean that about 13% of patients with nil or low pre-treatment PSMA expression receiving Lu-PSMA therapy which they are unlikely to respond to, potentially costing more in the long term..

[H1]WB-MRI and its changing landscape in prostate cancer

Whole-body MRI is showing increasing promise as an 'all-in-one' modality for cancer diagnosis and staging without the need for radiation exposure. Interest in this technique is growing for use across different cancer sites; in multiple myeloma WB-MRI is an established modality for skeletal assessment. Some studies have shown higher sensitivity of WB-MRI compared to 18FDG-PET-CT for the detection of both focal and diffuse bone involvement.[105]

WB-MRI is now being developed for routine clinical use in prostate cancer[106]. In a study assessing the diagnostic accuracy of WB-MRI in newly diagnosed intermediate-risk and high-risk disease[20], the mean sensitivity and specificity for N1 disease were 1.00 and 0.96, respectively, whereas for M1b disease, the mean sensitivity and specificity were 0.90 and 0.88, respectively. In a subgroup of 53 patientswith biochemical recurrence after local treatment, the overall sensitivity and specificity of WB-MRI were 0.94 and 0.83, respectively, and the sensitivity and specificity at bone, lymph node and visceral levels were 1.00 and 0.91, 0.79 and 0.97 and 0.60 and 1.00, respectively.[107] In addition, interobserver reliability has been shown to be high: in a prospective cohort study of 56 patients, WB-MRI imaging data were reviewed by two radiologists, showing that WB-MRI had an interobserver concordance (κ) of 0.79, 0.68, and 0.58 for N1, M1a, and M1b diseases, respectively[20]. The Advanced Prostate Cancer Consensus Conference (APCCC) and the EAU have recognised that WB-MRI is more sensitive than conventional imaging techniques for detecting bone metastases, hence providing alternative methods other than PET based imaging for disease assessment . Current advances in WB-MRI sequence acquisitions are now making it feasible to acquire WB-MRI scans in less than 60 minutes, which helps to reduce patient waiting times, anxiety and potentially increase the efficiency of WB-MRI as a next generation imaging technique [108].

Data on cancer detection rates in localised prostate cancer are limited, possibly because WB-MRI is not the initial modality used for diagnosis and/or surveillance at early stages of prostate cancer and the research and clinical interests are concentrated around staging and/or detection of metastases. Thus, cancer detection rate for localised prostate cancer was not included in studies[20,107]

[H2]Sequences commonly used in WB-MRI

Common and routinely used sequences in WB-MRI include T1-weighted, T2-weighted, diffusion-weighted imaging and Dixon imaging[109] . Dixon sequence is a chemical shift-based technique that enables fat-only and water-only images, providing improved lesion conspicuity as well as fat quantification in malignant and benign tissues.

[H2]**Standardisation of WB-MRI acquisition, interpretation and reporting**

Patient-specific and disease-specific standardisation of WB-MRI protocol has been addressed by the UK Quantitative WB-DWI Technical Workgroup, METRADS-P[110] and MY-RADS[43], which involved a panel of experts with experience in physics, clinical imaging and oncology and provided recommendations to promote standardisation and reduce variabilities in image acquisition, qualitative interpretation and reporting of WB-MRI.

The interobserver repeatability of radiologists' reporting using MET-RADS-P (Table 3) has been evaluated in one study[111] in which two independent radiologists, a board-certified senior radiologist with 9 years experience and a resident with 6 months training were asked to report 50 consecutive paired WB-MRI examinations. The senior radiologist reported 249 metastatic regions compared with 251 by the resident. For the MET-RADS-P primary RAC pattern assessment, excellent agreement was seen for many regions including the cervical, dorsal and lumbosacral spine, as well as the pelvis, limbs, lungs and other sites (κ 0.81- 1.0). Substantial agreement was seen for thorax, retroperitoneal nodes, other nodes and the liver (κ 0.61 - 0.80). Similarly, substantial agreement was reported for the secondary RAC pattern for cervical (κ 0.93) and retroperitoneal nodes (κ 0.89) and moderate agreement for dorsal spine, pelvis, thorax, limbs and pelvic nodes(κ 0.61-0.80)[111].

[H2]Superparamagnetic iron oxide nanoparticles

Use of superparamagnetic iron oxide (SPIO) nanoparticles, including ultrasmall particles of iron oxide (USPIO) has been shown to further enhance accuracy for nodal disease assessment in prostate cancer[112-116] These agents are taken up by normal lymph nodes leading to a T2 shortening effect and meaning that these normal nodes appear low in signal on MRI, whereas, by contrast, abnormal lymph nodes with low uptake of the agent would remain high in signal intensity. Limited data exists comparing the use of SPIO MRI with PET-CT[117], but a 2021 head-to-head comparison with 68Ga PSMA PET-CT showed overall higher nodal detection using SPIO MRI but with a substantial discordance rate[118]. These data illustrate the potential complementary roles of the modalities, but use of SPIO MRI is limited due to its availability, lack of regulatory approval in some jurisdictions and the skill set required for its implementation. For instance SPIO has been reported to cause local infusion site inflammation and can cause a systemic complement activation-related reaction when injected too rapidly[119] . The FDA recommends its use under continuous blood pressure monitoring[119].The role of SPIO MRI in prostate cancer assessment in the WB-MRI setting and beyond nodal assessment requires further evidence before its role can be truly defined[115]. Whether using

this technique could augment (or even interfere with) assessment of the primary lesion and non-nodal metastases is yet to be explored[120,121].

[H2]WB-MRI derived markers

Imaging biomarkers derived from WB-MRI include ADC, signal fat fraction (sFF) and proton density fraction (PDFF), which quantify tissue features (water diffusion and fat content respectively) and thus provide information that characterises disease states.

[H3]ADC for assessing bone metastases

DWI can enable categorisation of treatment response in prostate cancer bone using ADC values, whereas bone scintigraphy and CT are only able to identify disease progression[122] . .ADC also known as apparent diffusion coefficient is a biomarker derived from DWI which could help quantify the diffusivity of water molecules in extracellular compartment of biological tissues. Diffusion of water is restricted with increased cellularity within tissue as seen in cancers thus leading to low ADC. The reverse is seen in normal cells or in cellular necrosis, which in turn permits increased diffusivity of water between cells and hence a high ADC [123,124]. Studies have shown that the mean and median bone ADC values increase following response to treatment[125,126,41]. Similar findings have been demonstrated regarding bone involvement in other cancers such as multiple myeloma, breast, pancreatic and colorectal cancers [126,127]. Spatial heterogeneity is seen within the metastasis, with the centre of the lesion having a greater increase in ADC values compared to periphery. This spatial heterogeneity can be assessed by performing whole-tumour volumetric texture analysis on ADC maps, facilitating the monitoring of treatment response[126].

[H3]Signal fat fraction and proton density fat fraction

According to the RECIST v1.1 criteria, a pathological node must meet the criterion of a short axis of diameter of ≥15mm on CT[38]. However, 10–20% of normal-sized lymph nodes will contain tumour deposits and 30% of enlarged nodes are benign[129]; furthermore, normal structures and other pathological processes can mimic nodal disease.

Signal fat fraction (sFF) and proton density fat fraction (PDFF) are quantitative imaging biomarkers under investigation that estimate tissue fat content. Normal lymph nodes are composed of a fatty hilum surrounded by a cellular rim[130]. This hilar fat is often lost in metastatic infiltration . The in-phase and out-of-phase images on the Dixon sequence can be used to generate fat-only and water-only images, which could then be used to calculate the signal fat fraction. [131,132]. Adeleke et al. showed that mean sFF was significantly lower for PET-positive (0.63) compared with negative nodes (0.79) ($p<0.0001$) in patients with radio-recurrent prostate cancer. 131Similarly, Appayya et al. demonstrated that the mean FF was lower in PET-positive (mean FF= 43.1%) than in PET-negative (mean FF= 59.2%) nodes ($p<0.001$)132.In addition, sFF can act as a quantitative measure for treatment response. In an analysis of 28 lymph nodes across 13 patients who had received ADT, the baseline median sFF was lower in treatment responders than patients in the non-responder group[133]. PDFF is also useful in assessing vertebral bone marrow lesions to distinguish benign lesions from bone marrow metastases— in a retrospective review of 192 spinal MRI examinations, PDFF values were significantly lower in benign vertebral bone marrow lesions compared with metastases1[34].

[H1]Limitations of WB-MRI

Although many studies have demonstrated the superior performance of WB-MRI over established diagnostic methods such as CT and bone scan, a number of challenges to implementation remain. The main disadvantages of WB-MRI include the relatively long acquisition times and contraindication in certain patient sub-groups. Imaging distortion and

motion artefacts, differential diagnosis of findings, incidentalomas and limited availability of WB-MRI technology still remain some of its major challenges

[H2]Metallic implants, scan duration & claustrophobia.

Although MRI is an imaging modality with excellent tissue resolution and no radiation exposure, it can be inconvenient to patients. The duration of a WB-MRI scan is long — 40-60 minutes on average. This long reporting time for each individual scan means this could further lengthen time to treatment decisions. and reduce accessibility to the scan due to the limited capacity of radiology departments to perform MRI scans at any given time.

The use of MRI is contraindicated in patients with metal implants that are labelled as MRI-unsafe[135], owing to risk of heating or implants becoming dislodged causing MRI projectile injuries. MR-conditional implants could be scanned only under very specific conditions provided in their labelling. Metal implants could also cause image distortion around the metal due to distortion to the magnetic field homogeneity around the implant (Fig. 4). Approximately 5-30% of patients report distress when undergoing an MRI [136]. The relatively long acquisition time and the requirement to remain still can be anxiety-inducing to patients with claustrophobia, who might consequently acquire motion artefacts on their imaging, need sedation or alternative imaging methods in severe cases[136].

[H2]Limited Availability.

For a number of reasons, the availability of WB-MRI is currently limited. Performing WB-MRI examination requires MRI scanners with an adapted WB-MRI protocol, which is not available in every centre and sometimes needs MRI physics input to set up which is specialised and not always available;Furthermore, WB-MRI is not a commonly used technique, few (though growing number of) radiologists are trained to interpret WB-MRI examinations[137]. Finally, the relatively long duration of a WB-MRI scan means that many centres will currently struggle to routinely fit WB-MRI scans into their scan schedules.

[H2]Incidentalomas.

Several studies have shown that WB-MRI scans can lead to incidental finding of a malignancy or other finding[138,139,140]. A study that evaluated the clinical value of using WB-MRI for the health screening of the general adult population scanned 22 adults, and reported a range of incidental findings including one malignant lesion, and findings of unknown or no significance, most commonly hydroceles (in 61% of men), followed by benign bone lesions (32%) and others such as non-specific lymph nodes and cysts in various locations[139]. A separate study[140] reported that 32% of incidental findings on WB-MRI are potentially relevant and require subsequent investigation. These incidentalomas complicate communication with patients, especially when the risk of false positives might create unnecessary medical interventions and patient distress.

[H2]Image distortion on DWI and Dixon images.

When using DWI, Echo-planar imaging (EPI) has been the preferred pulse sequence for readout of diffusion-weighted data owing to its short imaging time and tolerance to motion[141]. However, EPI is very sensitive to inhomogeneities in the magnetic field such as the regions near the boundaries separating bone, fat and soft tissues, resulting in localised geometric distortion along the phase-encoding direction[142]. This distortion effect can also result in

misalignment of functional DWI imaging with anatomical imaging sequences by several millimetres[143], limiting its accuracy in the affected regions.

The Dixon method is a popular method for fat–water separation that relies on the chemical shift difference between water and fat[144]. However, presence of multiple and variable fat peaks within tissue of interest and magnetic field inhomogeneities, especially in regions of the body with air–tissue interfaces such as the head and neck, mean that fat-water inversion — in which fat-only and water-only voxels are swapped — can occur (Figure 5). This artefact affects 5–10% of Dixon MRIs[145]. Fat-water artefacts can mimic soft-tissue lesions and oedematous changes[146] and can also invalidate the quantitative measurement of the fat fraction[147,148].

[H2]Differential diagnosis of findings.

Although a modality with high sensitivity, some benign lesions detected on MRI could mimic malignancy, leading to false positives , unnecessary biopsies and inaccurate clinical assessments. Inflammation, such as from chronic prostatitis[149,150] or granulomatous prostatitis following BCG treatment[151], is known to mimic prostate cancer lesions on MRI. MRI can also cause false positive findings in the assessment of bone metastasis. MRI identifies bone metastases by detecting the replacement of the normal bone marrow content with neoplastic cells, which leads to alteration of the signal intensity on the morphological sequences and alteration of water diffusivity on DWI sequences[152]. Bone marrow reconversion is a process in which areas of yellow marrow are replaced by red marrow, usually occurring at times of physiological stress [153]. Bone marrow reconversion produces similar appearances to bone metastases on MRI and can be misleading in patients with malignant tumours[154,155].

[H1]Next generation imaging: implications for overall survival

Despite encouraging results regarding the accuracy of PSMA and WB-MRI, no large prospective, multicentre, randomised studies to date have demonstrated the superiority of WB-MRI compared with conventional imaging or head-to-head comparison of WB-MRI with PSMA, for improvement in overall survival or patient-reported outcome measures (PROMs). Although there is debate as to the necessity of producing such data in order to change practice for an imaging modality in prostate cancer. The ability to change clinical guidelines in favour of using these NGI over conventional imaging would be further strengthened by such studies demonstrating clinical benefit, improved patient survival, health economic benefit and improved PROMs.

Although PSMA PET is approved in an increasing number of settings[156], the research on its use focuses heavily on the diagnostic accuracy of the modality. PSMA PET has been shown to be more sensitive than conventional imaging and PSMA-avid lesions can be detected at very low PSA levels [15-19]. This discrepancy between imaging techniques can result in stage migration and a subsequent change in management plan for that patient. However, a change in management plan has not been demonstrated to translate to an increase in disease-free survival or overall survival. The biological and clinical significance of the presence of small PSMA-avid lesions remains unknown and, as a result, the upstaging of patients with small PSMA-avid lesions and potential change in their treatment away from radical therapy might deny these patients a chance of cure[157].

[H1]Cost and accessibility of PSMA versus MRI

In addition to their clinical benefits, cost and accessibility of PSMA PET and WB-MRI scans are also important factors in future implementation of these imaging modalities in routine clinical practice. This section explores the estimated costs involved in setting up and performing PSMA-PET and WB MRI scans, although formal health-economic analyses are awaited.

[H2]Cost of setup

Availability of PSMA PET radiotracers varies between countries according to factors including limited access to tracers, constrained scanner capacities and expertise. Most clinically used radiotracers are typically produced using a cyclotron, availability of which can be a limitation to its usage. However, Gallium-68 can be eluted from a radionuclide generator (a self-contained system housing an equilibrium mixture of a parent–daughter radionuclide pair, which is designed to provide the daughter radionuclide formed by the decay of the parent radionuclide) whereby the parent isotope Ge-68 can be decayed to produce Ga-68. This approach can be implemented in PET facilities that do not own a cyclotron[158].

The initial outlay cost of Ga-PSMA PET/CT is in the region of £150k–170k (USD$201k– $228k) owing to the cost of the system needed to generate the radioisotope, including a Gallium generator and cassette. The cassette needs to be replaced regularly, every 10–12 months on average. However, unlike Ga-68, other radiopharmaceuticals, including ^{18}F-DCPFyL and ^{18}F-PSMA-1007, have a longer half life[159] and thus the potential for centralised, large-scale production that can be distributed to sites without a cyclotron , which could reduce costs. Additional costs stem from the requirement for specialised trained nuclear medicine physicists to handle nuclear material. The handling, storage and disposal of ^{68}Ga-PSMA and other PSMA-conjugated radiotracers is regulated by government policies. Furthermore, the costs of safe disposal of nuclear material are relatively high in the USA and Europe. The average cost of a single PET/CT scanner ranges from USD$225k for basic 16-slice scanners to USD$750k for 64+ slice scanners with feature-rich images[160]. The hope is that as more data emerges , this could influence policy decisions around radioisotope usage and handling, making it more practical for widespread use.

For WB-MRI, a 1.5 T or 3T magnet scanner is required. The average cost of a new commercial MRI machine manufactured after 2009 is estimated at USD$3 million for a 1.5T scanner and at least $4.9 million for a 3T scanner [161] Factoring in installation costs and maintenance of the MRI suite, , the total cost can reach $3.6–6million[161,162]. However, many hospitals already have MRI scanners or have access to mobile imaging services that could be adapted to carry out WB-MRI examinations after installation of a WB-MRI software protocol.

[H2]Cost of a single scan

According to the NHS England reference cost dataset[163] one WB-MRI scan without contrast costs, on average, £202 ($270). Conventional imaging modalities such as bone scan and CT cost £288 ($386) and £117 ($157), respectively. No direct cost was listed in the NHS dataset] for a PSMA PET scan; however, a PET/CT scan involving more than three body areas costs £762 ($1,020) and a choline-PET test costs £884 ($1,184), and the cost of PSMA-PET would be expected to be similar to these, if not higher. A 2021 Australian health economic analysis using data from the proPSMA trial[164] estimated the cost of a single ^{68}Ga-PSMA PET scan to be AUD$1,203 (~GBP£648, $869), which is cheaper than the cost of conventional imaging (CT and bone scan) at AUD$1412(~GBP£760, $1019); however, this estimation is sensitive to the efficiency of the Gallium generator and, therefore, might only be generalisable to countries with local on-site production.

Considering the cost of set-up and individual scans, WB-MRI is likely to be cheaper overall than PSMA-PET; if WB-MRI were to replace the combination of conventional imaging techniques, this might confer a cost saving overall[8,9]. Formal health economic evaluation should be performed to compare PSMA PET/CT, WB-MRI and conventional imaging techniques.

The future roles of WB-MRI and PSMA PET-CT

For patients with biochemical relapsed disease after radical prostatectomy, PSMA has become the imaging modality of choice, where available. However, for relapse after radiotherapy with high serum PSA levels (>2 Ng/ml),PSMA PET, WB-MRI or even choline PET all have an active role. The result of an ongoing study[26] comparing the use of WB-MRI with ^{18}F-Choline PET in radiorecurrent disease is awaited .

For patients with hormone-sensitive, oligometastatic disease who might be amenable to metastasis-directed therapy, PSMA-PET has demonstrated disease detection and disease free survival superiority over PET scanning with choline and fluciclovine[165]. However, no single study of metastasis-directed therapy has used WB-MRI for patient identification during the enrollment process, possibly owing to lack of data[166,167]comparing the diagnostic accuracy of WB-MRI to PSMA or other NGI technologies in the setting of oligometastatic disease. The use of non-PET based NGI to offer alternative metastasis-directed therapy options in centres or patients who are unable to have a PSMA study due to lack of accessibility would be desirable in the future.

WB-MRI might have a major role in the poly-metastatic hormone-sensitive or mCRPC states, in which NGI might be indicated when disease progression is clinically suspected despite conventional imaging showing no changes, especially in patients with bone metastases. Taking into account the high sensitivity of the DWI protocol in the detection of bone metastases and evaluation of treatment response[168] plus the additional advantage of not requiring radiation, WB-MRI has some advantages over PSMA in this setting.

Well-designed, powered, randomized multicentre comparative studies would be desirable to assess the value of ^{68}Ga-PSMA PET, WB-MRI and conventional imaging for disease detection, disease burden evaluation and survival across different prostate cancer disease states, though equipoise and obtaining funding to run such studies is a challenge. In addition, , WB-MRI & PSMA-derived indices including ADC, sFF, PSMA-TV, and TL-PSMA should be evaluated, in order to better evaluate to patient outcomes.

Identification of the specific patient population who might benefit from metastasis-directed therapy is important and NGI will play a major role in this process. Accurate evaluation of disease and location is required before offering SABR and other focal metastasis-directed therapies to ensure the best oncological outcomes. Ideally, trials should evaluate differential outcomes in survival between patients treated based on CT, PSMA, WB-MRI and other NGIs. The next 5–10 years will be an exciting time for the health technological evaluation of these NGIs and other upcoming candidates.

[H1]Conclusions

The role of NGIs across the disease spectrum in prostate cancer is gradually evolving. With much of the emerging data supporting imaging techniques with improved diagnostic accuracy over standard-of-care imaging in the form of CT and bone scan. NGIs have an increasingly important role in disease staging. Two of these imaging modalities: PSMA PET-CT and WB-MRI show particular promise. However, their relative roles in patients with prostate cancer are yet to be fully defined and future studies that consider oncological outcomes would be desirable and may help to define their role for detection, disease burden evaluation and response monitoring across different prostate cancer disease states

Glossary

- (B0):The **B0** in MRI refers to the main static magnetic field (scanner magnetic field) used to polarize spins and is measured in teslas (T). The majority of MRI systems in clinical use are 1.5T or 3T.

- Echo-planar imaging (EPI): An MRI pulse sequence in which data for the entire image is collected following a single radiofrequency (RF) excitation. It has the advantage of rapid image acquisition but with poorer resolution.

Competing interests

The authors declare no competing interests.

References:

1. Global Cancer Observatory: Cancer Today. Lyon, France: International Agency for Research on Cancer. Available from: https://gco.iarc.fr/today, accessed [03/01/2022]
2. D'Amico AV, Whittington R, Malkowicz SB, et al. Biochemical Outcome After Radical Prostatectomy, External Beam Radiation Therapy, or Interstitial Radiation Therapy for Clinically Localized Prostate Cancer. JAMA. 1998;280(11):969–974.
3. van Leeuwen FWB, van der Poel HG. Oligometastases: the art of providing metastases-directed therapy in prostate cancer. Nat Rev Urol. 2022 May;19(5):259-260. doi: 10.1038/s41585-022-00570-9. PMID: 35075272.

4. Schatzl G, Madersbacher S, Thurridl T, Waldmüller J, Kramer G, Haitel A, Marberger M. High-grade prostate cancer is associated with low serum testosterone levels. Prostate. 2001 Apr;47(1):52-8. doi: 10.1002/pros.1046. PMID: 11304729.
5. Carceles-Cordon M, Kelly WK, Gomella L, Knudsen KE, Rodriguez-Bravo V, Domingo-Domenech J. Cellular rewiring in lethal prostate cancer: the architect of drug resistance. Nat Rev Urol. 2020 May;17(5):292-307. doi: 10.1038/s41585-020-0298-8. Epub 2020 Mar 16. PMID: 32203305; PMCID: PMC7218925.
6. Artibani W, Porcaro AB, De Marco V, Cerruto MA, Siracusano S. Management of Biochemical Recurrence after Primary Curative Treatment for Prostate Cancer: A Review. Urol Int. 2018;100(3):251-262. doi: 10.1159/000481438. Epub 2017 Nov 21. PMID: 29161715.
7. Conteduca V, Poti G, Caroli P, et al. Flare phenomenon in prostate cancer: recent evidence on new drugs and next generation imaging. Ther Adv Med Oncol. 2021;13:1758835920987654. Published 2021 Feb 24. doi:10.1177/1758835920987654
8. Taylor SA et al. Streamline investigators. Diagnostic accuracy of whole-body MRI versus standard imaging pathways for metastatic disease in newly diagnosed non-small-cell lung cancer: the prospective Streamline L trial. Lancet Respir Med. 2019 Jun;7(6):523-532. doi: 10.1016/S2213-2600(19)30090-6.
9. Taylor SA et al. Streamline investigators. Diagnostic accuracy of whole-body MRI versus standard imaging pathways for metastatic disease in newly diagnosed colorectal cancer: the prospective Streamline C trial. Lancet Gastroenterol Hepatol. 2019 Jul;4(7):529-537.
10. Messiou C et al. Prospective Evaluation of Whole-Body MRI versus FDG PET/CT for Lesion Detection in Participants with Myeloma. Radiol Imaging Cancer. 2021 Sep;3(5):e210048.
11. Tikkinen KAO et al. Prostate cancer screening with prostate-specific antigen (PSA) test: a clinical practice guideline. BMJ. 2018 Sep 5;362:k3581.
12. Kohestani K, Chilov M, Carlsson SV. Prostate cancer screening-when to start and how to screen?. Transl Androl Urol. 2018;7(1):34-45. doi:10.21037/tau.2017.12.25
13. O'Sullivan JM, Norman AR, Cook GJ, Fisher C, Dearnaley DP. Broadening the criteria for avoiding staging bone scans in prostate cancer: a retrospective study of patients at the Royal Marsden Hospital. BJU Int. (2003) 92:685–9. doi: 10.1046/j.1464-410X.2003.04480.x
14. Trabulsi EJ et al. Optimum Imaging Strategies for Advanced Prostate Cancer: ASCO Guideline. J Clin Oncol. 2020 Jun 10;38(17):1963-1996.
15. Hofman MS et al. Prostate-specific membrane antigen PET-CT in patients with high-risk prostate cancer before curative-intent surgery or radiotherapy (proPSMA): a prospective, randomised, multicentre study. Lancet. 2020 Apr 11;395(10231):1208-1216.
16. F. Ceci, C. Uprimny, B. Nilica, et al.(68)Ga-PSMA PET/CT for restaging recurrent prostate cancer: which factors are associated with PET/CT detection rate? Eur J Nucl Med Mol Imaging, 42 (2015), pp. 1284-1294
17. Peng L et al. Can 68Ga-prostate specific membrane antigen positron emission tomography/computerized tomography provide an accurate lymph node staging for patients with medium/high risk prostate cancer? A diagnostic meta-analysis. Radiat Oncol. 2020 Oct 1;15(1):227.
18. Petersen LJ, Zacho HD. PSMA PET for primary lymph node staging of intermediate and high-risk prostate cancer: an expedited systematic review. Cancer Imaging. 2020 Jan 23;20(1):10.
19. Rahman, L.A., Rutagengwa, D., Lin, P. et al. High negative predictive value of 68Ga PSMA PET-CT for local lymph node metastases in high risk primary prostate cancer with histopathological correlation. Cancer Imaging 19, 86 (2019).
20. Johnston EW et al. Multiparametric whole-body 3.0-T MRI in newly diagnosed intermediate- and high-risk prostate cancer: diagnostic accuracy and interobserver agreement for nodal and metastatic staging. Eur Radiol. 2019 Jun;29(6):3159-3169.
21. Lecouvet FE et al. Can whole-body magnetic resonance imaging with diffusion-weighted imaging replace Tc 99m bone scanning and computed tomography for single-step detection

of metastases in patients with high-risk prostate cancer? Eur Urol. 2012 Jul;62(1):68-75. doi: 10.1016/j.eururo.2012.02.020. Epub 2012 Feb 17.
22. Kesch C, Kratochwil C, Mier W, Kopka K, Giesel FL. 68Ga or 18F for Prostate Cancer Imaging? J Nucl Med. 2017 May;58(5):687-688. doi: 10.2967/jnumed.117.190157. Epub 2017 Apr 13. PMID: 28408526.
23. Raveenthiran, S., Yaxley, J., Gianduzzo, T. *et al.* The use of ^{68}Ga-PET/CT PSMA to determine patterns of disease for biochemically recurrent prostate cancer following primary radiotherapy. *Prostate Cancer Prostatic Dis* **22,** 385–390 (2019).
24. Bluemel C et al. 68Ga-PSMA-PET/CT in Patients With Biochemical Prostate Cancer Recurrence and Negative ^{18}F-Choline-PET/CT. Clin Nucl Med. 2016 Jul;41(7):515-21.
25. Sawicki LM et al. Prospective comparison of whole-body MRI and 68Ga-PSMA PET/CT for the detection of biochemical recurrence of prostate cancer after radical prostatectomy. Eur J Nucl Med Mol Imaging. 2019 Jul;46(7):1542-1550.
26. Adeleke S et al. Localising occult prostate cancer metastasis with advanced imaging techniques (LOCATE trial): a prospective cohort, observational diagnostic accuracy trial investigating whole-body magnetic resonance imaging in radio-recurrent prostate cancer. BMC Med Imaging. 2019 Nov 15;19(1):90.
27. Palma DA et al. Stereotactic Ablative Radiotherapy for the Comprehensive Treatment of Oligometastatic Cancers: Long-Term Results of the SABR-COMET Phase II Randomized Trial. J Clin Oncol. 2020 Sep 1;38(25):2830-2838.
28. Ost P et al. Surveillance or Metastasis-Directed Therapy for Oligometastatic Prostate Cancer Recurrence: A Prospective, Randomized, Multicenter Phase II Trial. J Clin Oncol. 2018 Feb 10;36(5):446-453.
29. Chalkidou A et al. Stereotactic ablative body radiotherapy in patients with oligometastatic cancers: a prospective, registry-based, single-arm, observational, evaluation study. Lancet Oncol. 2021 Jan;22(1):98-106.
30. Phillips R, Shi WY, Deek M, et al. Outcomes of Observation vs Stereotactic Ablative Radiation for Oligometastatic Prostate Cancer: The ORIOLE Phase 2 Randomized Clinical Trial. JAMA Oncol. 2020;6(5):650–659.
31. Guckenberger M et al. Characterisation and classification of oligometastatic disease: a European Society for Radiotherapy and Oncology and European Organisation for Research and Treatment of Cancer consensus recommendation. Lancet Oncol. 2020 Jan;21(1):e18-e28.
32. Lievens Y et al. Defining oligometastatic disease from a radiation oncology perspective: An ESTRO-ASTRO consensus document. Radiother Oncol. 2020 Jul;148:157-166.
33. Foster, Corey C. MD, MS; Pitroda, Sean P. MD; Weichselbaum, Ralph R. MD Definition, Biology, and History of Oligometastatic and Oligoprogressive Disease, The Cancer Journal: 3/4 2020 - Volume 26 - Issue 2 - p 96-99
34. Sweeney CJ et al. Chemohormonal Therapy in Metastatic Hormone-Sensitive Prostate Cancer. N Engl J Med. 2015 Aug 20;373(8):737-46.
35. Lecouvet FE et al. Use of modern imaging methods to facilitate trials of metastasis-directed therapy for oligometastatic disease in prostate cancer: a consensus recommendation from the EORTC Imaging Group. Lancet Oncol. 2018 Oct;19(10):e534-e545.
36. Gillessen S et al. Management of Patients with Advanced Prostate Cancer: Report of the Advanced Prostate Cancer Consensus Conference 2019. Eur Urol. 2020 Apr;77(4):508-547.
37. Aggarwal, R., Romero, G.R., Friedl, V. *et al.* Clinical and genomic characterization of Low PSA Secretors: a unique subset of metastatic castration resistant prostate cancer. *Prostate Cancer Prostatic Dis* **24,** 81–87 (2021).
38. Eisenhauer EA, Therasse P, Bogaerts J. et al.New response evaluation criteria in solid tumours: revised RECIST guideline (version 1.1) Eur J Cancer. 2009;45:228–247

39. Scher HI et al. Trial design and objectives for castration-resistant prostate cancer: updated recommendations from the prostate cancer clinical trials working group 3. J Clin Oncol. 2016;34:1402–18.
40. Seitz, A.K., Rauscher, I., Haller, B. *et al.* Preliminary results on response assessment using ^{68}Ga-HBED-CC-PSMA PET/CT in patients with metastatic prostate cancer undergoing docetaxel chemotherapy. *Eur J Nucl Med Mol Imaging* **45,** 602–612 (2018).
41. Blackledge MD et al. Assessment of treatment response by total tumor volume and global apparent diffusion coefficient using diffusion-weighted MRI in patients with metastatic bone disease: a feasibility study. PLoS One. 2014 Apr 7;9(4):e91779.
42. Turpin A et al. Imaging for Metastasis in Prostate Cancer: A Review of the Literature. Front Oncol. 2020 Jan 31;10:55. doi: 10.3389/fonc.2020.00055.
43. Messiou C et al. Guidelines for Acquisition, Interpretation, and Reporting of Whole-Body MRI in Myeloma: Myeloma Response Assessment and Diagnosis System (MY-RADS). Radiology. 2019 Apr;291(1):5-13. doi: 10.1148/radiol.2019181949.
44. Maurer T, Eiber M, Schwaiger M, Gschwend JE. Current use of PSMA-PET in prostate cancer management. Nat Rev Urol. 2016 Apr;13(4):226-35. doi: 10.1038/nrurol.2016.26. Epub 2016 Feb 23. PMID: 26902337.
45. van der Sar, E.C.A., van Kalmthout, L.M. & Lam, M.G.E.H. PSMA PET/CT in primary prostate cancer diagnostics: an overview of the literature. *Tijdschr Urol* **10,** 101–108 (2020).
46. Eder M et al. Novel Preclinical and Radiopharmaceutical Aspects of [68Ga]Ga-PSMA-HBED-CC: A New PET Tracer for Imaging of Prostate Cancer. Pharmaceuticals (Basel). 2014 Jun 30;7(7):779-96.
47. Afshar-Oromieh A et al. PET imaging with a [68Ga]gallium-labelled PSMA ligand for the diagnosis of prostate cancer: biodistribution in humans and first evaluation of tumour lesions. Eur J Nucl Med Mol Imaging. 2013 Apr;40(4):486-95. Erratum in: Eur J Nucl Med Mol Imaging. 2013 May;40(5):797-8.
48. Andaglia G et al. Distribution of metastatic sites in patients with prostate cancer: A population-based analysis. Prostate. 2014 Feb;74(2):210-6. doi: 10.1002/pros.22742. Epub 2013 Oct 16. PMID: 24132735.
49. Kamaleshwaran KK, Mittal BR, Harisankar CN, Bhattacharya A, Singh SK, Mandal AK. Predictive value of serum prostate specific antigen in detecting bone metastasis in prostate cancer patients using bone scintigraphy. Indian J Nucl Med. 2012;27(2):81-84.
50. Guo Y, Wang L, Hu J, Feng D, Xu L. Diagnostic performance of choline PET/CT for the detection of bone metastasis in prostate cancer: A systematic review and meta-analysis. PLoS One. 2018;13(9):e0203400. Published 2018 Sep 7.
51. T. Lengana, I.O. Lawal, T.G. Boshomane, et al. 68Ga-PSMA PET/CT replacing bone scan in the initial staging of skeletal metastasis in prostate cancer: a fait accompli? Clin Genitourin Cancer, 16 (2018), pp. 392-401
52. von Eyben FE, Picchio M, von Eyben R, Rhee H, Bauman G. 68Ga-Labeled Prostate-specific Membrane Antigen Ligand Positron Emission Tomography/Computed Tomography for Prostate Cancer: A Systematic Review and Meta-analysis. Eur Urol Focus. 2018 Sep;4(5):686-693.
53. Perera M et al. Gallium-68 Prostate-specific Membrane Antigen Positron Emission Tomography in Advanced Prostate Cancer-Updated Diagnostic Utility, Sensitivity, Specificity, and Distribution of Prostate-specific Membrane Antigen-avid Lesions: A Systematic Review and Meta-analysis. Eur Urol. 2020 Apr;77(4):403-417.
54. Afshar-Oromieh A et al. Comparison of PET imaging with a (68)Ga-labelled PSMA ligand and (18)F-choline-based PET/CT for the diagnosis of recurrent prostate cancer. Eur J Nucl Med Mol Imaging. 2014 Jan;41(1):11-20.

55. Morigi JJ et al. Prospective Comparison of ^{18}F-Fluoromethylcholine Versus 68Ga-PSMA PET/CT in Prostate Cancer Patients Who Have Rising PSA After Curative Treatment and Are Being Considered for Targeted Therapy. J Nucl Med. 2015 Aug;56(8):1185-90.
56. Glicksman RM et al. [18F]DCFPyL PET-MRI/CT for unveiling a molecularly defined oligorecurrent prostate cancer state amenable for curative-intent ablative therapy: study protocol for a phase II trial. BMJ Open. 2020 Apr 22;10(4):e035959.

57. Efficacy of [18F]PSMA-1007 PET/CT in Patients With Biochemial Recurrent Prostate Cancer. https://clinicaltrials.gov/ct2/show/record/NCT04742361?view=record accessed 27/05/22.

---

58. Aksu A, Karahan Şen NP, Tuna EB, Aslan G, Çapa Kaya G. Evaluation of 68Ga-PSMA PET/CT with volumetric parameters for staging of prostate cancer patients. Nucl Med Commun. 2021 Feb 5.
59. Zou Q et al. Semi-automatic evaluation of baseline whole-body tumor burden as an imaging biomarker of 68Ga-PSMA-11 PET/CT in newly diagnosed prostate cancer. Abdom Radiol (NY). 2020 Dec;45(12):4202-4213.
60. Karyagar SS, Karyagar S, Guven O. Correlations of the 68Ga-PSMA PET/CT derived primary prostate tumor PSMA expression parameters and metastatic patterns in patients with Gleason Score >7 prostate cancer. Hell J Nucl Med. 2020 May-Aug;23(2):120-124.
61. Yildirim ÖA, Gündoğan C, Can C, Poyraz K, Erdur E, Kömek H. Correlations between whole body volumetric parameters of 68Ga-PSMA PET/CT and biochemical-histopathological parameters in castration-naive and resistant prostate cancer patients. Ann Nucl Med. 2021 Feb 14.
62. Acar E, Özdoğan Ö, Aksu A, Derebek E, Bekiş R, Çapa Kaya G. The use of molecular volumetric parameters for the evaluation of Lu-177 PSMA I&T therapy response and survival. Ann Nucl Med. 2019 Sep;33(9):681-688.
63. Schmidkonz C et al. 68Ga-PSMA-11 PET/CT-derived metabolic parameters for determination of whole-body tumor burden and treatment response in prostate cancer. Eur J Nucl Med Mol Imaging. 2018 Oct;45(11):1862-1872.
64. Michalski K, Mix M, Meyer PT, Ruf J. Determination of whole-body tumour burden on [68Ga]PSMA-11 PET/CT for response assessment of [177Lu]PSMA-617 radioligand therapy: a retrospective analysis of serum PSA level and imaging derived parameters before and after two cycles of therapy. Nuklearmedizin. 2019 Dec;58(6):443-450. English.
65. Has Simsek D et al. Can PSMA-based tumor burden predict response to docetaxel treatment in metastatic castration-resistant prostate cancer? Ann Nucl Med. 2021 Mar 30.
66. Wahl RL, Jacene H, Kasamon Y, Lodge MA. From RECIST to PERCIST: evolving considerations for PET response criteria in solid tumors. J Nucl Med. 2009;50(Suppl 1):122S–1250.
67. Gupta M, Choudhury PS, Rawal S, Goel HC, Rao SA. Evaluation of RECIST, PERCIST, EORTC, and MDA Criteria for Assessing Treatment Response with Ga68-PSMA PET-CT in Metastatic Prostate Cancer Patient with Biochemical Progression: a Comparative Study [published correction appears in Nucl Med Mol Imaging. 2020 Oct;54(5):267]. Nucl Med Mol Imaging. 2018;52(6):420-429.

68. Lawhn-Heath C et al. Prostate-specific Membrane Antigen PET in Prostate Cancer. Radiology. 2021 May;299(2):248-260.

69. Ceci F et al. E-PSMA: the EANM standardized reporting guidelines v1.0 for PSMA-PET. Eur J Nucl Med Mol Imaging. 2021 May;48(5):1626-1638. doi: 10.1007/s00259-021-05245-y. Epub 2021 Feb 19. PMID: 33604691; PMCID: PMC8113168

70. Vierasu I, Trotta N, Albisinni S, et al. Clinical experience with 18F-JK-PSMA-7 when using a digital PET/CT. Eur J Hybrid Imaging. 2022;6(1):6. Published 2022 Mar 15. doi:10.1186/s41824-022-00128-3

71. Bodar, Y. et al. Prospective analysis of clinically significant prostate cancer detection with [18F]DCFPyL PET/MRI compared to multiparametric MRI: a comparison with the histopathology in the radical prostatectomy specimen, the ProStaPET study. European journal of nuclear medicine and molecular imaging, 49(5), 1731–1742.

72. Krohn T et al. [(68)ga]psma-hbed uptake mimicking lymph node metastasis in coeliac ganglia: An important pitfall in clinical practice. Eur J Nucl Med Mol Imaging 42(2): 210-214, 2015
73. Bialek EJ, Malkowski B. Celiac ganglia: can they be misinterpreted on multimodal 68Ga-PSMA-11 PET/MR? Nucl Med Commun. 2019 Feb;40(2):175-184.
74. de Galiza Barbosa, F., Queiroz, M.A., Nunes, R.F. et al. Nonprostatic diseases on PSMA PET imaging: a spectrum of benign and malignant findings. Cancer Imaging 20, 23 (2020).
75. Gykiere P, Goethals L, Everaert H. Healing Sacral Fracture Masquerading as Metastatic Bone Disease on a 68Ga-PSMA PET/CT. Clin Nucl Med. 2016 Jul;41(7):e346-7.
76. Kanthan, Gowri L. et al. Follicular Thyroid Adenoma Showing Avid Uptake on 68Ga PSMA-HBED-CC PET/CT, Clinical Nuclear Medicine: April 2016 - Volume 41 - Issue 4 - p 331-332
77. Radzina, Maija et al. “Accuracy of 68Ga-PSMA-11 PET/CT and multiparametric MRI for the detection of local tumor and lymph node metastases in early biochemical recurrence of prostate cancer.” American journal of nuclear medicine and molecular imaging vol. 10,2 106-118. 15 Apr. 2020
78. Iravani A et al.^{68}Ga PSMA-11 PET with CT urography protocol in the initial staging and biochemical relapse of prostate cancer. Cancer Imaging. 2017 Dec 21;17(1):31. doi: 10.1186/s40644-017-0133-5. PMID: 29268784; PMCID: PMC5740783.
79. Kroenke M et al. Matched-Pair Comparison of ^{68}Ga-PSMA-11 and ^{18}F-rhPSMA-7 PET/CT in Patients with Primary and Biochemical Recurrence of Prostate Cancer: Frequency of Non-Tumor-Related Uptake and Tumor Positivity. J Nucl Med. 2021 Aug 1;62(8):1082-1088.
80. Dietlein F et al. Intraindividual Comparison of ^{18}F-PSMA-1007 with Renally Excreted PSMA Ligands for PSMA PET Imaging in Patients with Relapsed Prostate Cancer. J Nucl Med. 2020 May;61(5):729-734. doi: 10.2967/jnumed.119.234898.
81. Ghadanfer L, Usmani S, Marafi F, Al-Kandari F, Rasheed R. Incremental Value of Post Diuretic 68Ga-PSMA-11 PET-CT in Characterization of Indeterminate lLesions in Prostate Cancer. Asian Pac J Cancer Prev. 2020;21(12):3719-3723. Published 2020 Dec 1. doi:10.31557/APJCP.2020.21.12.3719
82. Morawitz J et al.. Is there a diagnostic benefit of late-phase abdomino-pelvic PET/CT after urination as part of whole-body 68 Ga-PSMA-11 PET/CT for restaging patients with biochemical recurrence of prostate cancer after radical prostatectomy? EJNMMI Res. 2022 Mar 4;12(1):12. doi: 10.1186/s13550-022-00885-z. PMID: 35244791; PMCID: PMC8897520.
83. Afshar-Oromieh A et al. The Clinical Impact of Additional Late PET/CT Imaging with 68Ga-PSMA-11 (HBED-CC) in the Diagnosis of Prostate Cancer. J Nucl Med. 2017 May;58(5):750-755. doi: 10.2967/jnumed.116.183483. Epub 2017 Jan 6. PMID: 28062595.
84. Hoffmann MA et al. Dual-Time Point [68Ga]Ga-PSMA-11 PET/CT Hybrid Imaging for Staging and Restaging of Prostate Cancer. Cancers (Basel). 2020 Sep 28;12(10):2788. doi: 10.3390/cancers12102788. PMID: 32998432; PMCID: PMC7600341.
85. Perveen G et al. Role of Early Dynamic Positron Emission Tomography/Computed Tomography with 68Ga-prostate-specific Membrane Antigen-HBED-CC in Patients with Adenocarcinoma Prostate: Initial Results. Indian J Nucl Med. 2018 Apr-Jun;33(2):112-117. doi: 10.4103/ijnm.IJNM_8_18. PMID: 29643670; PMCID: PMC5883427.

86. Uprimny C et al. Early dynamic imaging in 68Ga- PSMA-11 PET/CT allows discrimination of urinary bladder activity and prostate cancer lesions. Eur J Nucl Med Mol Imaging. 2017 May;44(5):765-775. doi: 10.1007/s00259-016-3578-z. Epub 2016 Nov 29. PMID: 27900519.
87. Freitag MT et al. Local recurrence of prostate cancer after radical prostatectomy is at risk to be missed in ^{68}Ga-PSMA-11-PET of PET/CT and PET/MRI: comparison with mpMRI integrated in simultaneous PET/MRI. Eur J Nucl Med Mol Imaging. 2017 May;44(5):776-787.
88. Burger IA et al. ^{68}Ga-PSMA-11 PET/MR Detects Local Recurrence Occult on mpMRI in Prostate Cancer Patients After HIFU. J Nucl Med. 2019 Aug;60(8):1118-1123.
89. Wright GL Jr, Grob BM, Haley C, et al. Upregulation of prostate-specific membrane antigen after androgen-deprivation therapy.Urology. 1996;48(2):326–34.
90. Evans MJ, Smith-Jones PM, Wongvipat J, et al. Noninvasive measurement of androgen receptor signaling with a positron-emitting radiopharmaceutical that targets prostate-specific membrane antigen. Proc Natl Acad Sci USA. 2011;108:9578–9582.
91. Hope TA et al. 68Ga-PSMA-11 PET Imaging of Response to Androgen Receptor Inhibition: First Human Experience. J Nucl Med. 2017 Jan;58(1):81-84.
92. Murga JD et al. Synergistic co-targeting of prostate-specific membrane antigen and androgen receptor in prostate cancer. Prostate. 2015;75(3):242–54.
93. Afshar-Oromieh A, Debus N, Uhrig M, Hope TA, Evans MJ, Holland-Letz T, Giesel FL, Kopka K, Hadaschik B, Kratochwil C, Haberkorn U. Impact of long-term androgen deprivation therapy on PSMA ligand PET/CT in patients with castration-sensitive prostate cancer. Eur J Nucl Med Mol Imaging. 2018 Nov;45(12):2045-2054. doi: 10.1007/s00259-018-4079-z. Epub 2018 Jul 7. PMID: 29980832; PMCID: PMC6182397
94. Afshar-Oromieh A, Holland-Letz T, Giesel FL, Kratochwil C, Mier W, Haufe S, et al. Diagnostic performance of (68)Ga-PSMA-11 (HBED-CC) PET/CT in patients with recurrent prostate cancer: evaluation in 1007 patients. Eur J Nucl Med Mol Imaging. 2017;44:1258–68.
95. Emmett L et al. Rapid Modulation of PSMA Expression by Androgen Deprivation: Serial 68Ga-PSMA-11 PET in Men with Hormone-Sensitive and Castrate-Resistant Prostate Cancer Commencing Androgen Blockade. J Nucl Med. 2019 Jul;60(7):950-954.
96. Plouznikoff N et al. Evaluation of PSMA expression changes on PET/CT before and after initiation of novel antiandrogen drugs (enzalutamide or abiraterone) in metastatic castration-resistant prostate cancer patients. Ann Nucl Med. 2019 Dec;33(12):945-954.
97. US National Library of Medicine. ClinicalTrials.gov 2020. https://clinicaltrials.gov/ct2/show/NCT03876912 (accessed 03/01/2022)
98. Hofman MS, Hicks RJ, Maurer T, Eiber M. Prostate-specific Membrane Antigen PET: Clinical Utility in Prostate Cancer, Normal Patterns, Pearls, and Pitfalls. Radiographics. 2018 Jan-Feb;38(1):200-217
99. Rischpler C et al. 68Ga-PSMA-HBED-CC Uptake in Cervical, Celiac, and Sacral Ganglia as an Important Pitfall in Prostate Cancer PET Imaging. J Nucl Med. 2018 Sep;59(9):1406-1411.
100. Public Health England: Ionising radiation and you https://www.phe-protectionservices.org.uk/radiationandyou/ - accessed on 03/1/2022.
101. Siva S, Udovicich C, Tran B, Zargar H, Murphy DG, Hofman MS. Expanding the role of small-molecule PSMA ligands beyond PET staging of prostate cancer. Nat Rev Urol. 2020 Feb;17(2):107-118. doi: 10.1038/s41585-019-0272-5. Epub 2020 Jan 14. PMID: 31937920.
102. Hofman MS et al. TheraP Trial Investigators and the Australian and New Zealand Urogenital and Prostate Cancer Trials Group. [177Lu]Lu-PSMA-617 versus cabazitaxel in patients with metastatic castration-resistant prostate cancer (TheraP): a randomised, open-label, phase 2 trial. Lancet. 2021 Feb 27;397(10276):797-804.
103. Sartor O et al. VISION Investigators. Lutetium-177-PSMA-617 for Metastatic Castration-Resistant Prostate Cancer. N Engl J Med. 2021 Jun 23.

104. Transformative prostate cancer therapy 'should not be accepted' without PET imaginghttps://www.healthimaging.com/topics/medical-imaging/molecular-imaging/prostate-cancer-therapy-not-be-accepted-without-pet accessed 25/5/22
105. Ormond Filho AG et al. Whole-Body Imaging of Multiple Myeloma: Diagnostic Criteria. Radiographics. 2019 Jul-Aug;39(4):1077-1097.
106. Pasoglou V, Michoux N, Tombal B, Lecouvet F. Optimising TNM Staging of Patients with Prostate Cancer Using WB-MRI. J Belg Soc Radiol. 2016 Nov 19;100(1):101
107. Van Damme J et al. Comparison of ^{68}Ga-Prostate Specific Membrane Antigen (PSMA) Positron Emission Tomography Computed Tomography (PET-CT) and Whole-Body Magnetic Resonance Imaging (WB-MRI) with Diffusion Sequences (DWI) in the Staging of Advanced Prostate Cancer. Cancers (Basel). 2021 Oct 21;13(21):5286.
108. Lecouvet FE et al. Shortening the acquisition time of whole-body MRI: 3D T1 gradient echo Dixon vs fast spin echo for metastatic screening in prostate cancer. Eur Radiol. 2020 Jun;30(6):3083-3093.
109. Bitar R et al. P. MR pulse sequences: what every radiologist wants to know but is afraid to ask. Radiographics. 2006 Mar-Apr;26(2):513-37. doi: 10.1148/rg.262055063. PMID: 16549614.
110. Padhani AR et al. METastasis Reporting and Data System for Prostate Cancer: Practical Guidelines for Acquisition, Interpretation, and Reporting of Whole-body Magnetic Resonance Imaging-based Evaluations of Multiorgan Involvement in Advanced Prostate Cancer. Eur Urol. 2017 Jan;71(1):81-92.
111. Pricolo, P., Ancona, E., Summers, P. *et al.* Whole-body magnetic resonance imaging (WB-MRI) reporting with the METastasis Reporting and Data System for Prostate Cancer (MET-RADS-P): inter-observer agreement between readers of different expertise levels. *Cancer Imaging* **20,** 77 (2020).
112. Harisinghani MG et al. Ferumoxtran-10-enhanced MR lymphangiography: does contrast-enhanced imaging alone suffice for accurate lymph node characterization? AJR Am J Roentgenol. 2006 Jan;186(1):144-8.
113. Heesakkers RA et al. MRI with a lymph-node-specific contrast agent as an alternative to CT scan and lymph-node dissection in patients with prostate cancer: a prospective multicohort study. Lancet Oncol. 2008 Sep;9(9):850-6.
114. Thoeny HC et al. Combined ultrasmall superparamagnetic particles of iron oxide-enhanced and diffusion-weighted magnetic resonance imaging reliably detect pelvic lymph node metastases in normal-sized nodes of bladder and prostate cancer patients. Eur Urol. 2009 Apr;55(4):761-9.
115. Heesakkers RA et al. Prostate cancer: detection of lymph node metastases outside the routine surgical area with ferumoxtran-10-enhanced MR imaging. Radiology. 2009 May;251(2):408-14.
116. Meijer et al. High occurrence of aberrant lymph node spread on magnetic resonance lymphography in prostate cancer patients with a biochemical recurrence after radical prostatectomy. Int J Radiat Oncol Biol Phys. 2012 Mar 15;82(4):1405-10.
117. Fortuin AS et al. Value of PET/CT and MR lymphography in treatment of prostate cancer patients with lymph node metastases. Int J Radiat Oncol Biol Phys. 2012 Nov 1;84(3):712-8.
118. Schilham MGM et al. Head-to-Head Comparison of ^{68}Ga-Prostate-Specific Membrane Antigen PET/CT and Ferumoxtran-10-Enhanced MRI for the Diagnosis of Lymph Node Metastases in Prostate Cancer Patients. J Nucl Med. 2021 Sep 1;62(9):1258-1263.
119. Daldrup-Link HE. Ten Things You Might Not Know about Iron Oxide Nanoparticles. Radiology. 2017 Sep;284(3):616-629. doi: 10.1148/radiol.2017162759. PMID: 28825888; PMCID: PMC5584668.

120. Li CS, Harisinghani MG, Lin WC, Braschi M, Hahn PF, Mueller PR. Enhancement characteristics of ultrasmall superparamagnetic iron oxide particle within the prostate gland in patients with primary prostate cancer. J Comput Assist Tomogr. 2008 Jul-Aug;32(4):523-8.
121. Fukuda Y et al. Superparamagnetic iron oxide (SPIO) MRI contrast agent for bone marrow imaging: differentiating bone metastasis and osteomyelitis. Magn Reson Med Sci. 2006 Dec;5(4):191-6.
122. Padhani AR et al. Rationale for Modernising Imaging in Advanced Prostate Cancer. Eur Urol Focus. 2017 Apr;3(2-3):223-239.
123. Patterson DM, Padhani AR, Collins DJ. Technology insight: water diffusion MRI--a potential new biomarker of response to cancer therapy. Nat Clin Pract Oncol. 2008 Apr;5(4):220-33. doi: 10.1038/ncponc1073. Epub 2008 Feb 26. PMID: 18301415.
124. Padhani AR, Makris A, Gall P, Collins DJ, Tunariu N, de Bono JS. Therapy monitoring of skeletal metastases with whole-body diffusion MRI. J Magn Reson Imaging. 2014 May;39(5):1049-78. doi: 10.1002/jmri.24548. Epub 2014 Feb 10. PMID: 24510426.
125. Perez-Lopez R et al. Diffusion-weighted Imaging as a Treatment Response Biomarker for Evaluating Bone Metastases in Prostate Cancer: A Pilot Study. Radiology. 2017 Apr;283(1):168-177.
126. Reischauer C et al. Bone metastases from prostate cancer: assessing treatment response by using diffusion-weighted imaging and functional diffusion maps--initial observations. Radiology. 2010 Nov;257(2):523-31.
127. Jacobs, Michael A et al. “Multiparametric Whole-body MRI with Diffusion-weighted Imaging and ADC Mapping for the Identification of Visceral and Osseous Metastases From Solid Tumors.” Academic radiology vol. 25,11 (2018): 1405-1414. doi:10.1016/j.acra.2018.02.010
128. Dong H, Huang W, Ji X, Huang L, Zou D, Hao M, Deng S, Shen Z, Lu X, Wang J, Song Z, Zhang X, Xue H, Xia S. Prediction of Early Treatment Response in Multiple Myeloma Using MY-RADS Total Burden Score, ADC, and Fat Fraction From Whole-Body MRI: Impact of Anemia on Predictive Performance. AJR Am J Roentgenol. 2022 Feb;218(2):310-319. doi: 10.2214/AJR.21.26534. Epub 2021 Sep 15. PMID: 34523949.
129. Gross BH, Glazer GM, Orringer MB, Spizarny DL, Flint A. Bronchogenic carcinoma metastatic to normal-sized lymph nodes: frequency and significance. Radiology. 1988 Jan;166(1 Pt 1):71-4.
130. Ganeshalingam S, Koh DM. Nodal staging. Cancer Imaging. 2009;9(1):104-111. Published 2009 Dec 24. doi:10.1102/1470-7330.2009.0017
131. Adeleke S et al. Fat-fraction provides classification and treatment response assessment of metastatic lymph nodes for patients with radio-recurrent prostate cancer (Abstract) accessed from: https://discovery.ucl.ac.uk/id/eprint/10078201/1/Fat%20fraction%20abstract-Montreal%202019.pdf
132. Appayya et al. Quantitative mDixon Fat Fraction can differentiate metastatic nodes from benign nodes in prostate cancer patients (Abstract) accessed from: https://index.mirasmart.com/ISMRM2018/PDFfiles/0721.html
133. Cho SY et al. Biodistribution, tumor detection, and radiation dosimetry of ^{18}F-DCFBC, a low-molecular-weight inhibitor of prostate-specific membrane antigen, in patients with metastatic prostate cancer. J Nucl Med. 2012 Dec;53(12):1883-91.
134. Kwack KS, Lee HD, Jeon SW, Lee HY, Park S. Comparison of proton density fat fraction, simultaneous R2*, and apparent diffusion coefficient for assessment of focal vertebral bone marrow lesions. Clin Radiol. 2020 Feb;75(2):123-130.
135. Understand MRI safety labelling. https://www.fda.gov/media/101221/download accessed 29/05/22

136. Evans REC, Taylor SA, Kalasthry J, Sakai NS, Miles A; Streamline investigators. Patient deprivation and perceived scan burden negatively impact the quality of whole-body MRI. Clin Radiol. 2020 Apr;75(4):308-315.
137. Whole-body MRI can save money and stress, according to CTC study. https://www.ctc.ucl.ac.uk/ViewNews.aspx?Item=73. Accessed 03/01/2022.
138. Cieszanowski A, Maj E, Kulisiewicz P, et al. Non-contrast-enhanced whole-body magnetic resonance imaging in the general population: the incidence of abnormal findings in patients 50 years old and younger compared to older subjects. PLoS One. 2014;9(9):e107840. Published 2014 Sep 26.
139. Tarnoki DL, Tarnoki AD, Richter A, Karlinger K, Berczi V, Pickuth D. Clinical value of whole-body magnetic resonance imaging in health screening of general adult population. Radiol Oncol. 2015;49(1):10-16. Published 2015 Mar 3.
140. Hegenscheid K, Seipel R, Schmidt CO, Völzke H, Kühn JP, Biffar R, et al. Potentially relevant incidental findings on research whole-body MRI in the general adult population: frequencies and management. Eur Radiol. 2013;23:816–26.
141. Poustchi-Amin M, Mirowitz SA, Brown JJ, McKinstry RC, Li T. Principles and applications of echo-planar imaging: a review for the general radiologist. Radiographics. 2001 May-Jun;21(3):767-79.
142. Schallmo MP, Weldon KB, Burton PC, Sponheim SR, Olman CA. Assessing methods for geometric distortion compensation in 7 T gradient echo functional MRI data. Hum Brain Mapp. 2021 Sep;42(13):4205-4223.
143. Donato F Jr, Costa DN, Yuan Q, Rofsky NM, Lenkinski RE, Pedrosa I. Geometric distortion in diffusion-weighted MR imaging of the prostate-contributing factors and strategies for improvement. Acad Radiol. 2014 Jun;21(6):817-23.
144. Dixon WT. Simple proton spectroscopic imaging. Radiology. 1984 Oct;153(1):189-94.
145. Ben Glocker et al.Correction of Fat-Water Swaps in Dixon MRI https://www.doc.ic.ac.uk/~bglocker/pdfs/glocker2016.miccai.poster.pdf accessed on 30/4/22.
146. Kirchgesner, T., Acid, S., Perlepe, V. et al. Two-point Dixon fat-water swapping artifact: lesion mimicker at musculoskeletal T2-weighted MRI. Skeletal Radiol 49, 2081–2086 (2020).
147. Ladefoged, C.N et al. Impact of incorrect tissue classification in dixon-based MR-AC: fat-water tissue inversion. EJNMMI Phys 1(1) (2014) 101
148. Bray TJP, Chouhan MD, Punwani S, Bainbridge A, Hall-Craggs MA. Fat fraction mapping using magnetic resonance imaging: insight into pathophysiology. Br J Radiol 2017; 90: 20170344
149. Sciarra A et al. Magnetic resonance spectroscopic imaging (1H-MRSI) and dynamic contrast-enhanced magnetic resonance (DCE-MRI): pattern changes from inflammation to prostate cancer. Cancer Invest. 2010 May;28(4):424-32. doi: 10.3109/07357900903287048. PMID: 20073578.
150. Cheng Y, Zhang X, Ji Q, Shen W. Xanthogranulomatous prostatitis: multiparametric MRI appearances. Clin Imaging. 2014 Sep-Oct;38(5):755-7.
151. Suditu N, Negru D. Bacillus Calmette-Guérin therapy-associated granulomatous prostatitis mimicking prostate cancer on MRI: A case report and literature review. *Mol Clin Oncol*. 2015;3(1):249-251.
152. Lecouvet FE, Talbot JN, Messiou C, Bourguet P, Liu Y, de Souza NM; EORTC Imaging Group. Monitoring the response of bone metastases to treatment with Magnetic Resonance Imaging and nuclear medicine techniques: a review and position statement by the European Organisation for Research and Treatment of Cancer imaging group. Eur J Cancer. 2014 Oct;50(15):2519-31.

153. Małkiewicz A, Dziedzic M. Bone marrow reconversion - imaging of physiological changes in bone marrow. Pol J Radiol. 2012 Oct;77(4):45-50. doi: 10.12659/pjr.883628. PMID: 23269936; PMCID: PMC3529711.
154. Yu YS, Li WH, Li MH, Meng X, Kong LI, Yu JM. False-positive diagnosis of disease progression by magnetic resonance imaging for response assessment in prostate cancer with bone metastases: A case report and review of the pitfalls of images in the literature. *Oncol Lett*. 2015;10(6):3585-3590. doi:10.3892/ol.2015.3753
155. Tanaka T et al. A Case of Focal Bone Marrow Reconversion Mimicking Bone Metastasis: The Value of 111Indium Chloride. Acta Med Okayama. 2016 Aug;70(4):285-9.
156. EAU guideline of prostate cancer 2022. https://uroweb.org/guidelines/prostate-cancer accessed 29/05/22
157. Sundahl N, Gillessen S, Sweeney C, Ost P. When What You See Is Not Always What You Get: Raising the Bar of Evidence for New Diagnostic Imaging Modalities. Eur Urol. 2020 Aug 23:S0302-2838(20)30601-1.
158. Rodnick ME, Sollert C, Stark D, et al. Cyclotron-based production of 68Ga, [68Ga]GaCl3, and [68Ga]Ga-PSMA-11 from a liquid target. EJNMMI Radiopharm Chem. 2020;5(1):25. Published 2020 Nov 12.
159. Kesch C, Kratochwil C, Mier W, Kopka K, Giesel FL. 68Ga or 18F for Prostate Cancer Imaging? J Nucl Med. 2017 May;58(5):687-688. doi: 10.2967/jnumed.117.190157. Epub 2017 Apr 13. PMID: 28408526.
160. PET/CT price guide. source:https://info.blockimaging.com/bid/68875/how-much-does-a-pet-ct-scanner-cost. accessed on 03/01/2022.
161. How much does an MRI scanner cost: a complete overview. https://lbnmedical.com/how-much-does-an-mri-machine-cost/ accessed 29/5/22
162. Qin Cet al. Sustainable low-field cardiovascular magnetic resonance in changing healthcare systems. Eur Heart J Cardiovasc Imaging. 2022 Feb 14:jeab286
163. NHS England cost dataset. https://www.england.nhs.uk/national-cost-collection/ Accessed 03/01/2021.
164. de Feria Cardet RE et al. Is Prostate-specific Membrane Antigen Positron Emission Tomography/Computed Tomography Imaging Cost-effective in Prostate Cancer: An Analysis Informed by the proPSMA Trial. Eur Urol. 2021 Mar;79(3):413-418. doi: 10.1016/j.eururo.2020.11.043. Epub 2020 Dec 16.
165. Farolfi A et al. Positron Emission Tomography and Whole-body Magnetic Resonance Imaging for Metastasis-directed Therapy in Hormone-sensitive Oligometastatic Prostate Cancer After Primary Radical Treatment: A Systematic Review. Eur Urol Oncol. 2021 Mar 6:S2588-9311(21)00037-7.
166. Dyrberg E et al. 68Ga-PSMA-PET/CT in comparison with 18F-fluoride-PET/CT and whole-body MRI for the detection of bone metastases in patients with prostate cancer: a prospective diagnostic accuracy study. Eur Radiol. 2019 Mar;29(3):1221-1230. doi: 10.1007/s00330-018-5682-x. Epub 2018 Aug 21. PMID: 30132104.
167. Sawicki LM et al. Prospective comparison of whole-body MRI and 68Ga-PSMA PET/CT for the detection of biochemical recurrence of prostate cancer after radical prostatectomy. Eur J Nucl Med Mol Imaging. 2019 Jul;46(7):1542-1550. doi: 10.1007/s00259-019-04308-5. Epub 2019 Mar 16. PMID: 30879122.
168. Stecco A, Trisoglio A, Soligo E, Berardo S, Sukhovei L, Carriero A. Whole-Body MRI with Diffusion-Weighted Imaging in Bone Metastases: A Narrative Review. Diagnostics (Basel). 2018 Jul 9;8(3):45. doi: 10.3390/diagnostics8030045. PMID: 29987207; PMCID: PMC6163267.
169. Giesel FL et al. PSMA PET/CT with Glu-urea-Lys-(Ahx)-[^{68}Ga(HBED-CC)] versus 3D CT volumetric lymph node assessment in recurrent prostate cancer. Eur J Nucl Med Mol Imaging. 2015 Nov;42(12):1794-800.

170. Pernthaler B, Kulnik R, Gstettner C, Salamon S, Aigner RM, Kvaternik H. A Prospective Head-to-Head Comparison of 18F-Fluciclovine With 68Ga-PSMA-11 in Biochemical Recurrence of Prostate Cancer in PET/CT. Clin Nucl Med. 2019 Oct;44(10):e566-e573. doi: 10.1097/RLU.0000000000002703. PMID: 31283605.
171. Emmett L, Metser U, Bauman G, Hicks RJ, Weickhardt A, Davis ID, et al. Prospective, multisite, international comparison of 18F-fluoromethylcholine PET/CT, multiparametric MRI, and 68Ga-HBED-CC PSMA-11 PET/CT in men with high-risk features and biochemical failure after radical prostatectomy: clinical performance and patient outcomes. *J Nucl Med.* 2019;60:794–800. doi: 10.2967/jnumed.118.220103.
172. Morigi JJ, Stricker PD, van Leeuwen PJ, Tang R, Ho B, Nguyen Q, et al. Prospective comparison of 18F-Fluoromethylcholine versus 68Ga-PSMA PET/CT in prostate cancer patients who have rising PSA after curative treatment and are being considered for targeted therapy. *Journal of Nuclear Medicine.* 2015;56:1185–1190. doi: 10.2967/jnumed.115.160382.
173. Calais J, Ceci F, Eiber M, Hope TA, Hofman MS, Rischpler C, et al. 18F-fluciclovine PET-CT and 68Ga-PSMA-11 PET-CT in patients with early biochemical recurrence after prostatectomy: a prospective, single-centre, single-arm, comparative imaging trial. *The Lancet Oncology.* 2019;20:1286–1294
174. Schwenck J et al. Comparison of 68Ga-labelled PSMA-11 and 11C-choline in the detection of prostate cancer metastases by PET/CT. Eur J Nucl Med Mol Imaging. 2017 Jan;44(1):92-101. doi: 10.1007/s00259-016-3490-6. Epub 2016 Aug 24. PMID: 27557844.
175. Dietlein M et al. Comparison of [(18)F]DCFPyL and [(68)Ga]Ga-PSMA-HBED-CC for PSMA-PET Imaging in Patients with Relapsed Prostate Cancer. Mol Imaging Biol. 2015 Aug;17(4):575-84.
176. Szabo Z et al. Initial Evaluation of [(18)F]DCFPyL for Prostate-Specific Membrane Antigen (PSMA)-Targeted PET Imaging of Prostate Cancer. Mol Imaging Biol. 2015 Aug;17(4):565-74. doi: 10.1007/s11307-015-0850-8. PMID: 25896814; PMCID: PMC4531836.
177. Pienta KJ et al. A Phase 2/3 Prospective Multicenter Study of the Diagnostic Accuracy of Prostate Specific Membrane Antigen PET/CT with ^{18}F-DCFPyL in Prostate Cancer Patients (OSPREY). J Urol. 2021 Jul;206(1):52-61.
178. Morris MJ et al. CONDOR Study Group. Diagnostic Performance of ^{18}F-DCFPyL-PET/CT in Men with Biochemically Recurrent Prostate Cancer: Results from the CONDOR Phase III, Multicenter Study. Clin Cancer Res. 2021 Jul 1;27(13):3674-3682. doi: 10.1158/1078-0432.CCR-20-4573.
179. Behr SC et al. Phase I Study of CTT1057, an ^{18}F-Labeled Imaging Agent with Phosphoramidate Core Targeting Prostate-Specific Membrane Antigen in Prostate Cancer. J Nucl Med. 2019 Jul;60(7):910-916.
180. Turkbey B et al. ^{18}F-DCFBC Prostate-Specific Membrane Antigen-Targeted PET/CT Imaging in Localized Prostate Cancer: Correlation With Multiparametric MRI and Histopathology. Clin Nucl Med. 2017 Oct;42(10):735-740.
181. Cho SY et al. Biodistribution, tumor detection, and radiation dosimetry of ^{18}F-DCFBC, a low-molecular-weight inhibitor of prostate-specific membrane antigen, in patients with metastatic prostate cancer. J Nucl Med. 2012 Dec;53(12):1883-91.
182. Harmon SA et al. A Prospective Comparison of ^{18}F-Sodium Fluoride PET/CT and PSMA-Targeted 18F-DCFBC PET/CT in Metastatic Prostate Cancer. J Nucl Med. 2018 Nov;59(11):1665-1671.
183. Mena E et al. Clinical impact of PSMA-based ^{18}F-DCFBC PET/CT imaging in patients with biochemically recurrent prostate cancer after primary local therapy. Eur J Nucl Med Mol Imaging. 2018 Jan;45(1):4-11.
184. Rowe SP et al. ^{18}F-DCFBC PET/CT for PSMA-Based Detection and Characterization of Primary Prostate Cancer. J Nucl Med. 2015 Jul;56(7):1003-1010.

185. Hoberück S et al. Dual-time-point 64 Cu-PSMA-617-PET/CT in patients suffering from prostate cancer. J Labelled Comp Radiopharm. 2019 Jun 30;62(8):523-532.
186. Cantiello F et al. Comparison Between 64Cu-PSMA-617 PET/CT and 18F-Choline PET/CT Imaging in Early Diagnosis of Prostate Cancer Biochemical Recurrence. Clin Genitourin Cancer. 2018 Oct;16(5):385-391.
187. Giesel FL et al. Detection Efficacy of ^{18}F-PSMA-1007 PET/CT in 251 Patients with Biochemical Recurrence of Prostate Cancer After Radical Prostatectomy. J Nucl Med. 2019 Mar;60(3):362-368.
188. Malaspina S et al. Prospective comparison of ^{18}F-PSMA-1007 PET/CT, whole-body MRI and CT in primary nodal staging of unfavourable intermediate- and high-risk prostate cancer. Eur J Nucl Med Mol Imaging. 2021 Mar 13.
189. Dietlein F et al. Intraindividual Comparison of ^{18}F-PSMA-1007 with Renally Excreted PSMA Ligands for PSMA PET Imaging in Patients with Relapsed Prostate Cancer. J Nucl Med. 2020 May;61(5):729-734.
190. Alberts I et al. Comparing the clinical performance and cost efficacy of [^{68}Ga]Ga-PSMA-11 and [^{18}F]PSMA-1007 in the diagnosis of recurrent prostate cancer: a Markov chain decision analysis. Eur J Nucl Med Mol Imaging. 2021 Nov 13.
191. Witkowska-Patena E, Giżewska A, Miśko J, Dziuk M. 18F-Prostate-Specific Membrane Antigen 1007 and 18F-FCH PET/CT in Local Recurrence of Prostate Cancer. Clin Nucl Med. 2019 Jun;44(6):e401-e403. doi: 10.1097/RLU.0000000000002556. PMID: 30932984.
192. Derlin T et al. PSA-stratified detection rates for [68Ga]THP-PSMA, a novel probe for rapid kit-based 68Ga-labeling and PET imaging, in patients with biochemical recurrence after primary therapy for prostate cancer. Eur J Nucl Med Mol Imaging. 2018 Jun;45(6):913-922.
193. Afaq A et al. A Phase II, Open-label study to assess safety and management change using 68Ga-THP PSMA PET/CT in patients with high risk primary prostate cancer or biochemical recurrence after radical treatment: The PRONOUNCED study. J Nucl Med. 2021 Mar 19:jnumed.120.257527.
194. Kulkarni M et al. The management impact of 68gallium-tris(hydroxypyridinone) prostate-specific membrane antigen (68Ga-THP-PSMA) PET-CT imaging for high-risk and biochemically recurrent prostate cancer. Eur J Nucl Med Mol Imaging. 2020 Mar;47(3):674-686.
195. Bluemel C, Krebs M, Polat B, Linke F, Eiber M, Samnick S, et al. 68Ga-PSMA-PET/CT in patients with biochemical prostate cancer recurrence and negative 18F-choline-PET/CT. *Clin Nucl Med.* 2016;41:515–521.
196. Schmuck et al. Multiple Time-Point 68Ga-PSMA I&T PET/CT for Characterization of Primary Prostate Cancer, Clinical Nuclear Medicine: June 2017 - Volume 42 - Issue 6 - p e286-e293
197. Asokendaran ME, Meyrick DP, Skelly LA, Lenzo NP, Henderson A. Gallium-68 prostate-specific membrane antigen positron emission tomography/computed tomography compared with diagnostic computed tomography in relapsed prostate cancer. *World J Nucl Med*. 2019;18(3):232-237.
198. Oh SW et al. Quantitative and Qualitative Analyses of Biodistribution and PET Image Quality of a Novel Radiohybrid PSMA, ^{18}F-rhPSMA-7, in Patients with Prostate Cancer. J Nucl Med. 2020 May;61(5):702-709.
199. Hohberg M, Kobe C, Krapf P, et al. Biodistribution and radiation dosimetry of [18F]-JK-PSMA-7 as a novel prostate-specific membrane antigen-specific ligand for PET/CT imaging of prostate cancer. *EJNMMI Res*. 2019;9(1):66. Published 2019 Jul 25. doi:10.1186/s13550-019-0540-7
200. Dietlein, F., Mueller, P., Kobe, C. *et al.* [18F]-JK-PSMA-7 PET/CT Under Androgen Deprivation Therapy in Advanced Prostate Cancer. *Mol Imaging Biol* **23,** 277–286 (2021).

201. Piron S et al. Radiation Dosimetry and Biodistribution of ^{18}F-PSMA-11 for PET Imaging of Prostate Cancer. J Nucl Med. 2019 Dec;60(12):1736-1742.
202. Piron, S., De Man, K., Schelfhout, V. *et al.* Optimization of PET protocol and interrater reliability of ^{18}F-PSMA-11 imaging of prostate cancer. *EJNMMI Res* **10,** 14 (2020).
203. Schottelius M, Wurzer A, Wissmiller K, et al. Synthesis and Preclinical Characterization of the PSMA-Targeted Hybrid Tracer PSMA-I&F for Nuclear and Fluorescence Imaging of Prostate Cancer. J Nucl Med. 2019;60(1):71-78.
204. Depardon E et al. FDG PET/CT for prognostic stratification of patients with metastatic breast cancer treated with first line systemic therapy: Comparison of EORTC criteria and PERCIST. PLoS One. 2018 Jul 16;13(7):e0199529.

Table 1 | PSMA tracers in clinical use or preclinical development‡ **[Au: I have moved the columns around and reformatted the table to meet our House style – Thank you!]**

Study	Type of study (n)	Advantages	Limitations
^{68}Ga-HBED-CC or PSMA-11			

Hofman et al. [15] Giesel et al. [169] Pernthaler B et al[170] Emmett et al.[171] Morigi et al[172] Calais et al.[173] Schwenck et al.[174]	Randomised prospective study (n=302) Prospective analysis (n=21) Prospective analysis (n=58) Prospective, multisite study (n=91) Prospective study (n=38) Prospective study (n=50) Prospective study (n=123)	• More sensitive than CT based 3D volumetric lymph node evaluation in determining the node status of patients with recurrent prostate cancer • Significantly higher detection rate of prostate cancer lesions than ^{18}F-Fluciclovine, ^{11}C-Choline and ^{18}F-fluoromethylcholine	• Physiologic uptake on PET in cervical, celiac, and sacral ganglia of the sympathetic trunk • Accumulation of tracer in urinary bladder and thus less sensitive at detecting localised recurrence • Discordant findings of lymph node and bone lesions which may affect TNM staging

^{18}F-DCFPyL			
Dietlein et al.[175] Szabo et al.[176] Pienta et al.[177] Morris et al. [178]	Prospective comparative study (n=14) Prospective study (n=9) Prospective study, Phase II/III (n=385) Prospective, Phase III trial (n=208)	• Minimal non-target tissue uptake at or after 1h post injection • Higher mean SUV_{max} and tumour to background ratio compared to ^{68}Ga-HBED-CC • Labelling of PSMA tracers with ^{18}F offers advantages include improved image resolution, longer half-life, and increased production yields • Low hepatic uptake allowing the detection of liver lesions • Demonstrates disease localisation in the setting of negative standard imaging, resulting in change of intended management	• Reduced binding affinity *in vitro*
[^{18}F]CTT1057			
Behr et al.[179]	Phase I trial (n=20)	• Potentially lower radiation exposure of the kidneys and salivary glands	• Unexpectedly slow excretion kinetics - imaging at 90 minutes or later seems to be a prerequisite for high contrast imaging.

[^{18}F]DCFBC			
Turkbey B et al.[180] Cho et al.[181] Harmon et al.[182] Mena et al.[183] Rowe et al.[184]	Prospective analysis (n=13) Prospective analysis (n=5) Prospective analysis (n=28) Prospective study (n=41) Prospective study (n=13)	• Above a threshold PSA value of 0.78 ng/mL, ^{18}F-DCFBC was able to identify recurrence with high reliability. • Relatively low ^{18}F-DCFBC PET uptake in benign prostatic hypertrophy lesions, compared with cancer in the prostate, which may allow more specific detection	• Slow blood clearance and thus high background activity • Compared with ^{18}F-NaF PET/CT, ^{18}F-DCFBC PET/CT detected significantly fewer bone lesions in the setting of early or metastatic castrate-sensitive disease on treatment. • Sensitivity of ^{18}F-DCFBC for primary prostate cancer was less than MR imaging
^{64}Cu-PSMA-617			
Hoberück S et al.[185] Cantiello et al.[186]	Prospective study (n=16) Observational study (n=43)	• Easily synthesized, exhibit a favourable biodistribution in PSMA positive tumours • ^{64}Cu has imaging physics more similar to ^{18}F than ^{68}Ga - Better quality pictures on imaging	• Slow clearance for kidney and high liver uptake

		• More sensitive than ^{18}F PET/CT especially at low PSA values	
• **^{18}F-PSMA-1007**			
Giesel et al.[187] Malaspina et al. [188] Dietlein et al.[189] Alberts et al. [190] Witkowska-Patena et al [191]	Retrospective analysis (n=251) Prospective analysis (n=79) Prospective analysis (n=27) Retrospective analysis (n=244) Prospective study (n=40)	• Does not appear in the ureters and bladder within the imaging time interval – better delineation of local recurrence or pelvic lymph node metastasis • Greater sensitivity in nodal staging of primary prostate cancer than did WB-MRI with DWI or CT	• A higher liver uptake, which is caused by its higher lipophilicity • Uptake in muscle, submandibular and sublingual gland, spleen, pancreas, liver, and gallbladder • may decrease the interpretability of skeletal lesions compared to other renally excreted PSMA tracers. • significantly greater rates of uncertain findings and false positive findings when compared to ^{68}Ga-PSMA-11

[^{68}Ga] THP-PSMA			
Derlin et al.[192] Afaq A et al.[193] Kulkarni et al.[194]	Cohort study (n=25) Phase II trial (n=49) Prospective study (n=118)	• Stable in human serum for more than 6h and showed specific binding to PSMA-expressing cells • Simplified radiolabelling compared to other ^{68}Ga-PSMA conjugates • Safe to use with no serious adverse events • Influences clinical management in a significant number of patients	• Two incidences of minor adverse events (rash and pruritus)
68Ga-PSMA-I&T			

Bluemel et al. [195] Schmuck et al.[196] Asokendaran et al. [197]	Retrospective analysis (n=125) Prospective study (n=20) Retrospective analysis (n=150)	• ^{68}Ga-PSMA I&T PET/CT identified sites of recurrent disease in 43.8% of the patients with negative ^{18}F-choline PET/CT scans • Tracer uptake significantly higher in prostate cancer compared to other benign prostate tissue and the tumour to nontumour ratio increases overtime	No information found in literature to date
• **18F-rhPSMA-7**			
Oh et al.[198] Kroenke M et al.[79]	Retrospective analysis (n=202) Retrospective matched-pair comparison (n=160)	• An early imaging point (50-70 mins) is recommended for **18F-rhPSMA-7** to achieve highest imaging quality • Similar biodistribution to established PSMA glands and stable tumour uptake • Lower urinary excretion compared to ^{68}Ga-PSMA-11	• More frequent bone marrow uptake and increased negative impact on clinical decision making if uptake time is increased • Slightly more frequent uptake in benign areas compared to ^{68}Ga-PSMA-11
• **18F-JK-PSMA-7**			

Hohberg et al.[199] Dietlein et al[200]	Prospective study (n=10) Retrospective analysis (n=128)	• Fast excretion via blood in a similar order of magnitude to [^{18}F]-DCFPyL and reduced background enrichment • High detection rate in patients with PSA level greater than 0.3ng/ml under ADT	• Physiologic radiotracer accumulation in the salivary and lacrimal glands, liver, spleen, and intestines
18F-PSMA-11			
Piron et al. [201] Piron et al.[202]	Prospective study (n=6) Prospective study (n=44)	• Lower mean effective dose (12.8 ± 0.6 µSv/MBq), therefore lower total radiation dose than for other PSMA PET agents and in the same range as ^{18}F-DCFPyL	No information found in literature to date
PSMA-I&F (DOTAGA-k(Sulfo-Cy5)-y-nal-k-Sub-KuE)*			

Schottelius et al [203]	Preclinical study in mice and organ cryosections	• High affinity for PSMA and same for internalisation • Low accumulation in target organs • Can be conjugated with Sulfo-Cy5 dye and is thus useful for intraoperative guidance	No information found in literature to date

**Preclinical only*

‡*Table is non-exhaustive, with some of the less commonly applied tracers not included.*

Box 1 | PERCIST 1.0 Criteria of metabolic response

Progressive metabolic disease (PMD)

Increase of >30% in SUL_{peak} and absolute increase of $0.8SUL_{peak}$ units or a new FDG-avid lesion

Stable metabolic disease (SMD)

Response between PMD and PMR; no new lesions.

Partial metabolic response (PMR)

Reduction of >30% in SUL_{peak} and absolute drop of $0.8SUL_{peak}$ units.

Complete metabolic response

Complete resolution of FDG uptake within all lesions to a level ≤mean liver activity

FDG, fluorodeoxyglucose; SUL, standardised uptake value corrected for lean body mass; SUL_{peak}, peak SUL in a spherical $1cm^3$ volume of interest.

Figure 1: Clinical case demonstrating use of alternative PSMA tracers and PET MRI to identify disease recurrence in the vesicourethral junction region.

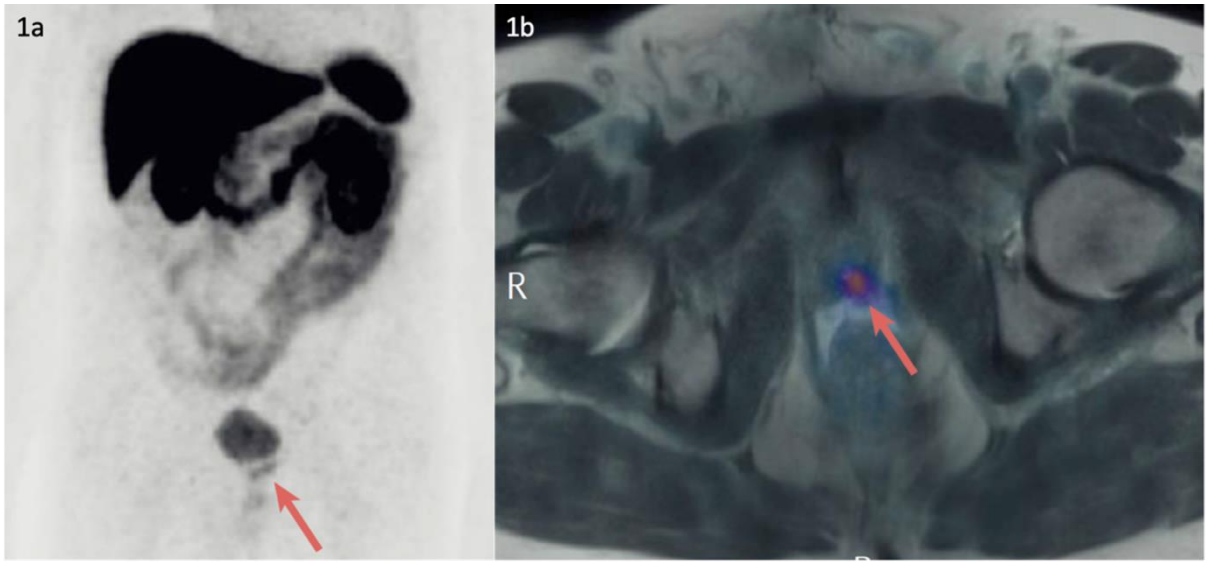

A 77-year-old man with an initial diagnosis of pT2 N0 Gleason 6 prostate adenocarcinoma, presenting with serum PSA 5ng/ml, and treated with prostatectomy 16 years ago. He now presents with biochemical recurrence with PSA 4.2 ng/ml, but negative CT and bone scan. ^{18}F-PSMA-1007 PETMRI scan shows a persistent focus of uptake (red arrow) at the left side of the bladder neck separate from the main bladder lumen on both maximum intensity projection (MIP) image (**1a**) and separate pelvic views (**1b**), suspicious of prostatectomy bed recurrence.

Figure 2: Clinical case demonstrating the use of alternative PSMA tracers and multiparametric MRI to identify disease recurrence in the vesicourethral junction region

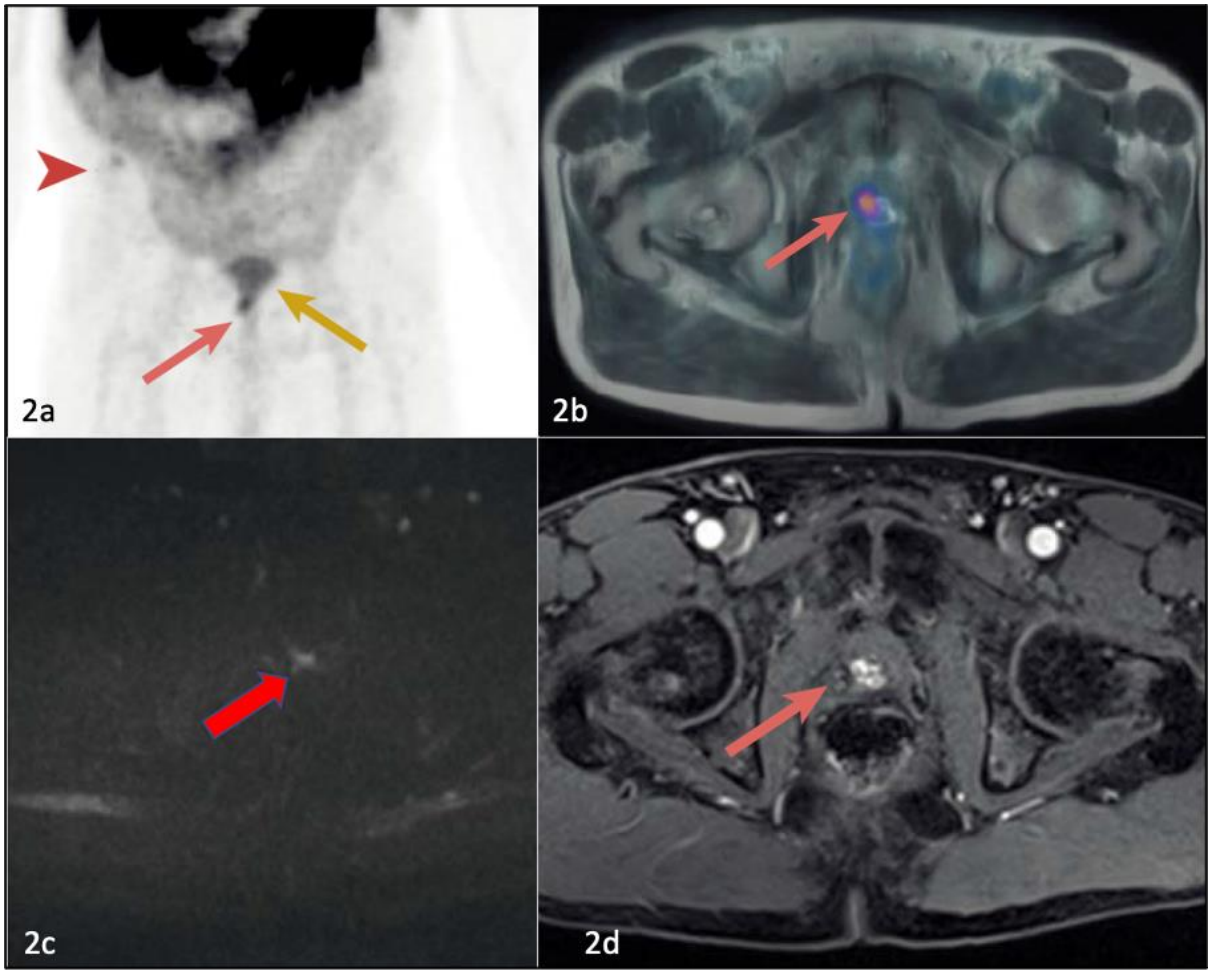

PSMA-PET MR (**2a, 2b**) and mpMRI images (**2c,2d**) from a 70- year -old man who underwent salvage radical prostatectomy (RALP) after initial HIFU. 2 months after RALP, serum PSA was 0.04 ug/L. Surgical resection was recorded as difficult but with a good end result and margins were clear on pathology. At 10 months after RALP, serum PSA had risen to 0.18ug/L and the 18F-PSMA-1007 PET MR study (**2a** and **2b**) demonstrated a focus of uptake at the bladder neck with added soft tissues on the right side (red arrow) suspicious for recurrence. 2a – maximum intensity projection (MIP) image; 2b - fused ^{68}Ga PSMA PET/CT, pelvic view. Note that the intensity is higher than excreted urine in the bladder lumen (yellow arrow).| There was also uptake at the right iliac crest (**2a**-red arrow head) with no clear morphological correlate, this was thought to be benign and incidental.

Dedicated mpMRI confirms soft tissues at prostate bed with possible restricted diffusion (**2c**-red arrow) and early enhancement (**2d**-red arrow). The patient underwent further cystoscopic resection. The lesion was confirmed to be benign prostatic tissue with no cancer identified. His serum PSA has not risen further since the resection.

Figure 3: Clinical cases demonstrating PSMA uptake in prostate cancer metastases and physiological variant uptake in ganglia

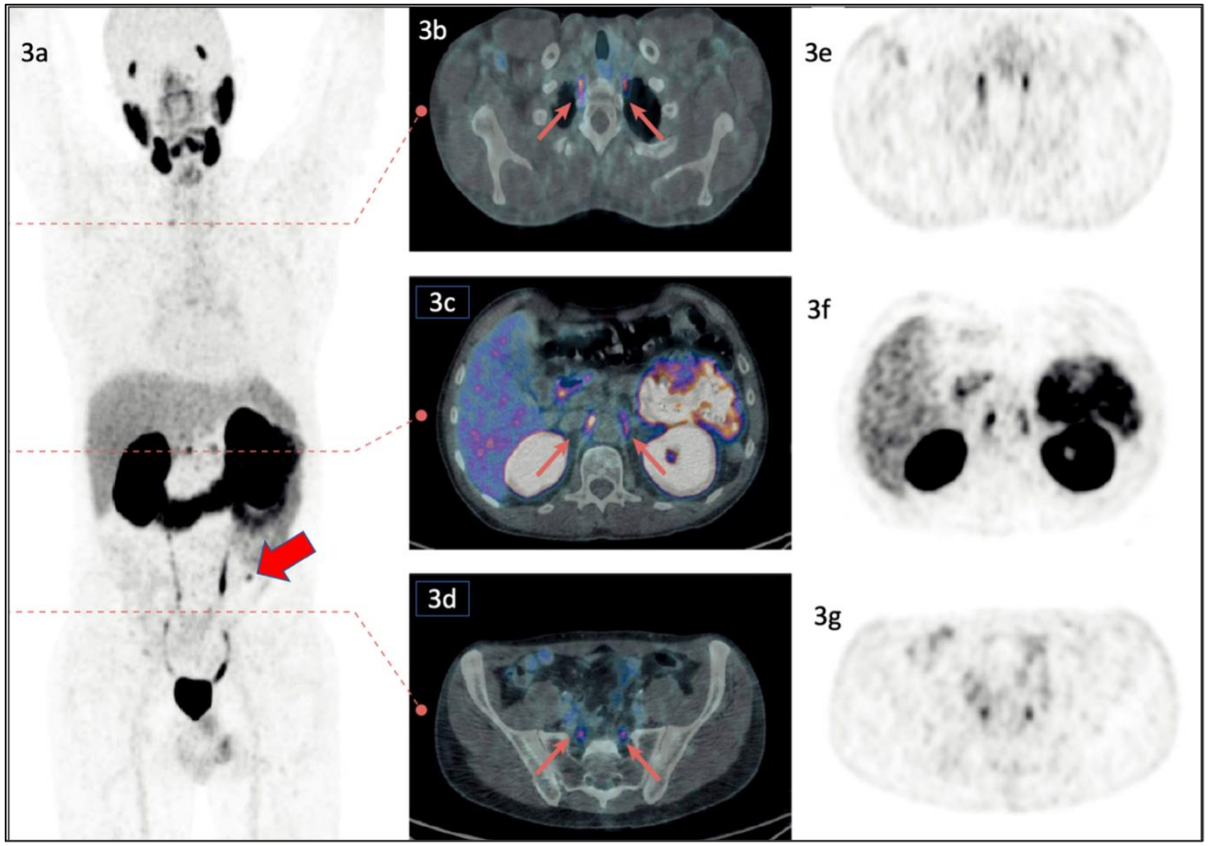

A 59-year-old male with biochemical recurrence post prostatectomy Ga^{68} PSMA PET (Fig **3a** MIP, Fig **3b-3d** axial PET-CT and Fig **3e-3g** axial PET images). There is a small left iliac bone metastasis on MIP images (**3a**-red arrow). Corresponding levels marked with red dotted lines on PET/CT images (**b-d**) and PET images(**e-g**) of the same patient. Paired red arrows indicate physiological PSMA uptake in (**b,e**) stellate, (**c,f**) coeliac and (**d, g**)sacral ganglia.

Figure 4| Motion artefact and image distortion around a metallic hip implant in WB-MRI.

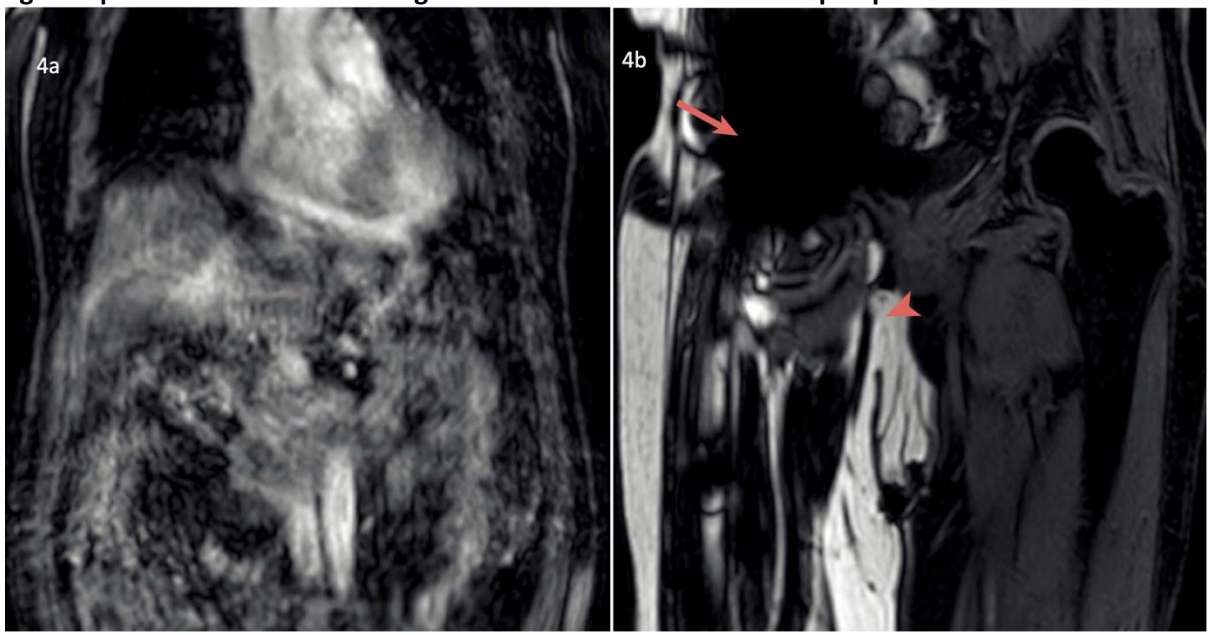

4a Motion artefact from physiological respiratory motion on WB-MRI in a patient with prostate cancer, coronal view, with blurring of the image.
4b Metallic implant artefact of right hip prosthesis (dark area with red arrow) on Dixon sequence, coronal view; there is also an area of fat-water swap (**4b** -red arrow head).

Figure 5: Fat-water swap artefacts in Dixon sequence in WB-MRI. Fat–water swap artefacts on Dixon sequences. Red arrows indicate regions or boundaries of fat–water swap

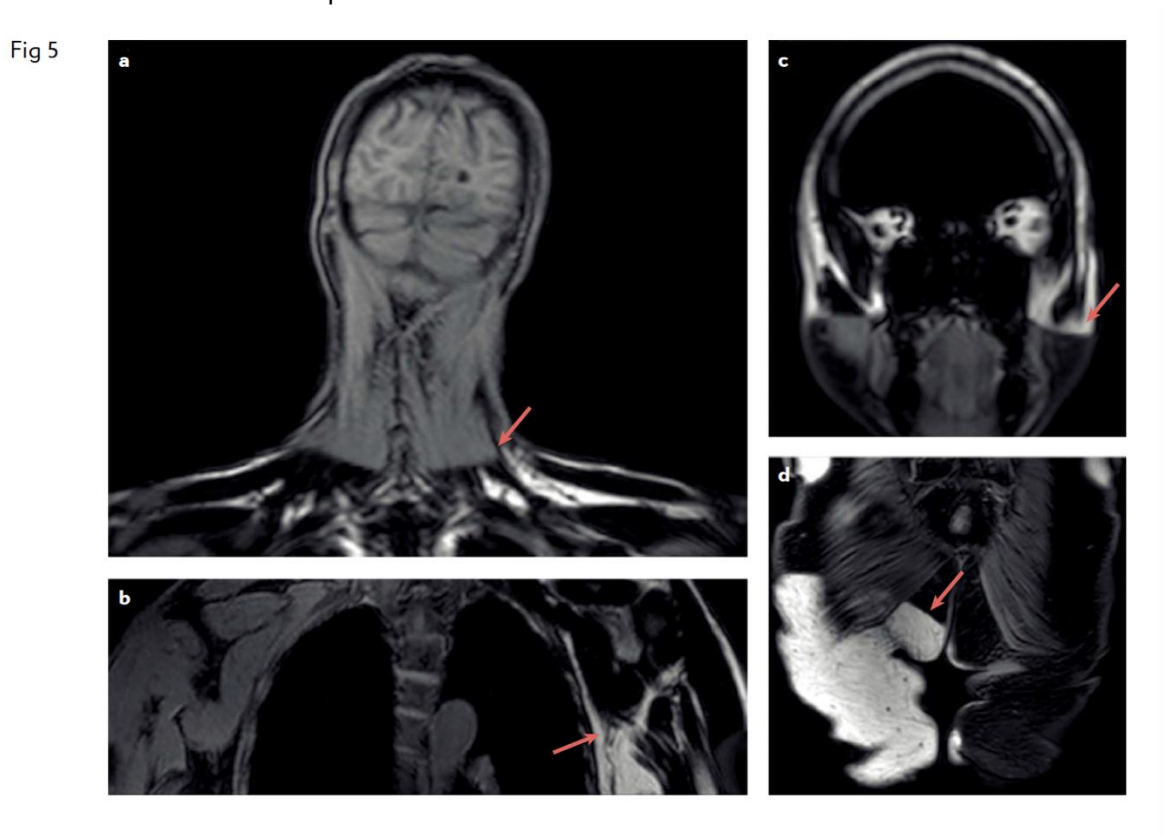

a) at the base of the neck
b) at the left arm
c) across the lower face
d) the right gluteal region